April 2018

A Novel Framework to Determine Physiological Signals From Blood Flow Dynamics

Prashanth Chetlur Adithya
University of South Florida, prashanthc@mail.usf.edu

A Novel Framework to Determine Physiological Signals From Blood Flow Dynamics

by

Prashanth Chetlur Adithya

A dissertation submitted in partial fulfillment
of the requirements for the degree of
Doctor of Philosophy in Electrical Engineering
Department of Electrical Engineering
College of Engineering
University of South Florida

Co-Major Professor: Ravi Sankar, Ph.D.
Co-Major Professor: Wilfrido A. Moreno, Ph.D.
Paris Wiley, Ph.D.
Andres Tejada-Martinez, Ph.D.
Stuart Hart, M.D.

Date of Approval:
March 14, 2018

Keywords: Blood flow sound, invasive blood pressure, heart rate, respiratory rate, multiresolution analysis, wavelet source separation, spectral subtraction, vital bio-signals, pattern recognition, cluster analysis, fetal phonocardiograms.

DEDICATION

To my parents, family, and friends. To Annabelle, for making this journey possible with your constant support and your invaluable feedback.

ACKNOWLEDGEMENTS

I would like to sincerely thank my advisors Dr. Ravi Sankar and Dr. Wilfrido Moreno for their constant support, guidance, and time throughout my research. I would like to graciously acknowledge Dr. Stuart Hart and his group at the USF Center for Advanced Medical Learning and Simulation for laying the foundation for this research and for extending the collaboration to perform animal studies. I would also like to recognize Mr. John Ringdahl and Mr. Ray Carr of OCCAM Technology Group for their contribution towards the development of the data acquisition system.

I am very grateful to Dr. Andres Tejada-Martinez for providing his invaluable feedback and continued collaboration in this research. I would like to thank Dr. Paris Wiley for providing his time and effort to be a part of this research. I would like to thank Dr. Fernando Falquez for supporting this collaboration initiative. I would like to recognize the importance of PhysioNet database and their reliable clinical datasets that enabled us to test the algorithms. I am very thankful to the Electrical Engineering Department and the Office of Innovative Education for providing the financial support that enabled me to complete the graduate program.

Mr. Kishore Kumar, thank you so much for expanding my understanding of fluid dynamics and time you have invested to generate a FLUENT simulation model. Ms. Shraddha, I cannot thank you enough for collaborating with me in my research and for expanding my knowledgebase with your invaluable discussions. Mr. Sai Bhardwaj thank you so much for your time.

TABLE OF CONTENTS

LIST OF TABLES

LIST OF FIGURES

ABSTRACT

Centers for Disease Control and Prevention (CDC) estimate that more than 11.2 million people require critical and emergency care in the United States per year [1]. Optimizing and improving patient morbidity and mortality outcomes are the primary objectives of monitoring in critical and emergency care. Patients in need of critical or emergency care in general are at a risk of single or multiple organ failures occurring due to a traumatic injury, a surgical event, or an underlying pathology that results in severe patient hemodynamic instability. Hence, continuous monitoring of fundamental cardiovascular hemodynamic parameters, such as heart rate, respiratory rate, blood pressure, blood oxygenation and core temperature, is essential to accomplish diagnostics in critical and emergency care. Today's standard of care measures these critical parameters using multiple monitoring technologies.

Though it is possible to measure all the fundamental cardiovascular hemodynamic parameters using the blood flow dynamics, its use is currently only limited to measuring continuous blood pressure. No other comparable studies in the literature were successful in quantifying other critical parameters from the blood flow dynamics for a few reasons. First, the blood flow dynamics exhibit a complicated and sensitive dynamic pressure field. Existing blood flow based data acquisition systems are unable to detect these sensitive variations in the pressure field. Further, the pressure field is also influenced by the presence of background acoustic interference, resulting in a noisy pressure profile. Thus in order to extract critical parameters from

this dynamic pressure field with fidelity, there is need for an integrated framework that is composed of a highly sensitive data acquisition system and advanced signal processing. In addition, existing state-of-the-art technologies require expensive instrumentation and complex infrastructure. The information sensed using these multiple monitoring technologies is integrated and visualized using a clinical information system. This process of integration and visualization creates the need for functional interoperability within the multiple monitoring technologies. Limited functional interoperability not only results in diagnostic errors but also their complexity makes it impossible to use such technologies to accomplish monitoring in low resource settings. These multiple monitoring technologies are neither portable nor scalable, in addition to inducing extreme patient discomfort. For these reasons, existing monitoring technologies do not efficiently meet the monitoring and diagnostic requirements of critical and emergency care.

In order to address the challenges presented by existing blood flow based data acquisition systems and other monitoring systems, a point of care monitoring device was developed to provide multiple critical parameters by means of uniquely measuring a physiological process. To demonstrate the usability of this novel catheter multiscope, a feasibility study was performed using an animal model. The corresponding results are presented in this dissertation. The developed measurement system first acquires the dynamics of blood flow through a minimally invasive catheter. Then, a signal processing framework is developed to characterize the blood flow dynamics and to provide critical parameters such as heart rate, respiratory rate, and blood pressure. The framework used to extract the physiological data corresponding to the acoustic field of the blood flow consisted of a noise cancellation technique and a wavelet based source separation. The preliminary results of the acoustic field of the blood flow revealed the presence of acoustic heart and respiratory pulses. A unique and novel framework was also developed to extract continuous

blood pressure from the pressure field of the blood flow. Finally, the computed heart and respiratory rates, systolic and diastolic pressures were benchmarked with actual values measured using conventional devices to validate the measurements of the catheter multiscope.

In summary, the results of the feasibility study showed that the novel catheter multiscope can provide critical parameters such as heart rate, respiratory rate and blood pressure with clinical accuracy. In addition, this dissertation also highlights the diagnostic potential of the developed catheter multiscope by presenting preliminary results of proof of concept studies performed for application case studies such as sinus rhythm pattern recognition and fetal monitoring through phonocardiography.

CHAPTER 1: INTRODUCTION

1.1 Background

Optimizing and improving patient morbidity and mortality outcomes are the primary objectives of monitoring in critical and emergency care. Patients in the need of critical or emergency care in general are at a risk of single or multiple organ failure occurring due to a traumatic injury, surgical event or an underlying pathology. This risk causes the patients to experience a hemodynamic instability. This hemodynamic instability further leads to ineffective circulating volume, cardiac function and/or vascular tone, ultimately resulting in an inadequate tissue oxygen delivery, end organ perfusion and death. Today's standard of care manages these instabilities by continuously monitoring various cardiovascular hemodynamic parameters (critical parameters) and thereby manipulating the macro and micro-circulation to improve tissue oxygen delivery [2] [3] [4]. Minimum standards of monitoring in critical and emergency care are specified by the college of intensive care medicine and they include continuous monitoring of fundamental critical parameters such as heart rate, respiratory rate, blood pressure (arterial and venous), blood oxygenation and core temperature [5]. From a systemic view, critical care monitoring can be summarized as a two stage process. At the first stage, multiple sensors acquire vital bio-signals corresponding to various physiological processes of the patient. At the second stage, a clinical information system is used to integrate and visualize the data from the multiple sensors used in first stage. State-of-the-art sensing technologies as shown in Figure 2.1, traditionally determine

critical parameters from the vital bio-signals, i.e., heart rate is determined either from Electrocardiogram (ECG) [6] or Photoplethysmograph (PPG) using 12 lead electrodes or a fingertip pulse oximetry; respiratory rate is determined either from respiratory flow or respiratory/lung sounds using a capnography or plethysmograph or a pneumatograph [7]; continuous blood pressure is determined by coupling the vascular pressures to an intravascular or extravascular pressure sensor through an arterial and/or venous catheter [8] [9]; blood oxygenation is determined from pulse oximetry [10] and core body temperature is measured using either a pulmonary arterial catheter or a urinary Foley catheter [11].

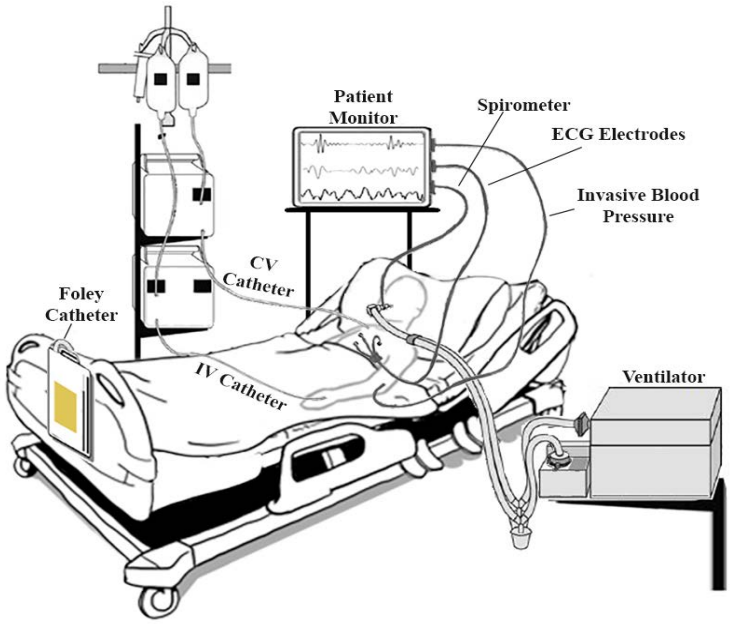

Figure 1.1: Multiple Vital Bio-signal Monitoring in Critical and Emergency Care. Image Adapted From [12].

1.2 Existing Challenges in Critical and Emergency Care Monitoring

Though it is possible to measure all the fundamental cardiovascular hemodynamic parameters such as heart rate, respiratory rate, blood oxygenation and core temperature from the blood flow, its use is currently only limited to measuring continuous blood pressure. No other comparable studies in the literature were successful in quantifying multiple critical parameters

from the blood flow dynamics for a few reasons. First, the blood flow dynamics exhibit a complicated and sensitive dynamic pressure field. Second, existing blood flow based data acquisition systems are unable to detect these sensitive variations within the dynamic pressure field. Further, the dynamic pressure field is influenced by the presence of acoustic waves, resulting in a noisy pressure profile. Thus in order to extract critical parameters from this dynamic pressure field with fidelity, there is need for an integrated framework that is composed of a highly sensitive data acquisition system and advanced signal processing. Even though monitoring heart rate and cardiac arrhythmia is traditionally done using a 12-lead ECG, recent research shows that morphological characteristics of ECG change due to electrolyte, water and other chemical changes in the cardiovascular system. This change in chemical composition has a direct influence on the electrical activity of the heart, resulting in false alarms and consequently, diagnostic errors. ECG is known for producing the highest quality measurement of heart rate, but it has been shown in the literature that heart rate measured from heart sounds is equally reliable as ECG [13]. Furthermore, the 12 lead ECG and the respiratory data acquisition systems cause extreme discomfort and restrict patient mobility. Although pulse oximetry is a gold standard monitoring technology for measuring blood oxygenation, the characteristics of the PPG signal are not fully understood among the medical community and it is still an area of active research [14] [15]. Also, blood oxygenation measurements of PPG are inaccurate when partial pressure levels of oxygen are high, and the inaccuracies also depend on properties of the skin which are highly subjective [16]. Further, core body temperature sensing technologies require the use of an additional catheter rather than using a preexisting arterial or venous line. Overall, the existing gold standard sensing technologies need multiple assessment systems in order to monitor critical cardiovascular hemodynamic parameters corresponding to various physiological processes. In addition, the existing clinical information

systems face limitations to achieve medical device interoperability, as accomplishing the integration and synchronization of various data acquisition systems used in the first stage is complicated. Existing information systems also do not acquire and store high resolution data. As a result, the complete morphology of the data acquired from various physiological sensors is not currently being used for clinical interventions. In addition, the current systems do not support the application of advanced data processing algorithms and consequently providing real time support for clinical decision making still remains as an unsolved challenge [17]. All the limitations of individual subsystems result in the following open challenges of critical and emergency care that need to be addressed.

- *Expensive Instrumentation and Complex Infrastructure:* To achieve minimum standards of care, heart rate, respiratory rate, blood pressure, blood oxygen saturation and core body temperature need to be continuously monitored as initial biomarkers of health status. This implicates that the, use of 12-lead ECG, Capnography, Arterial Catheter, Plethysmography and Foley Catheter is imperative. Not only these multiple monitoring technologies induce extreme patient discomfort, but also demand complex infrastructure in terms of hardware and software, in addition to being very expensive. For these reasons, current state-of-the-art critical monitoring technologies are ineffective and so in order to address this challenge of monitoring especially in low resource settings such as battlefields and emergency scenarios, a new approach is required.
- *Medical Device Interoperability:* In current critical and emergency care, vital bio-signals are acquired from myriad physiological sensing technologies. Due to most of these technologies being stand-alone devices, they do not integrate with each other creating a limited functional interoperability. This lack of functional interoperability leads to issues

associated to time synchronization of the data acquired from various physiological processes, eventually leading to diagnostic errors. In addition, due to the limited interoperability, critical care diagnostics is subject to high false alarm rate. Though many solutions have been proposed to address this issue, interoperability remains as an open challenge to date.

- *Portability and Scalability:* It has to be underlined that, existing critical and emergency care monitoring and diagnostic technologies are neither portable nor scalable. As a result, additional monitoring and diagnostic technologies are continuously brought in to meet the requirements of standard of care. The novel system presented in this work is portable, scalable and possibly applicable to multiple case studies of critical and emergency care.

1.3 Motivation and Research Objectives

Accomplishing monitoring from the dynamics of the blood flow is currently limited to measurement of continuous blood pressure. The hypothesis of this research is that, it is possible to extract other critical parameters such as heart rate, respiratory rate, blood oxygenation, and core temperature from the blood flow dynamics. Thus, our primary motivation of this research is to develop a novel point of care monitoring device that is capable of providing multiple critical

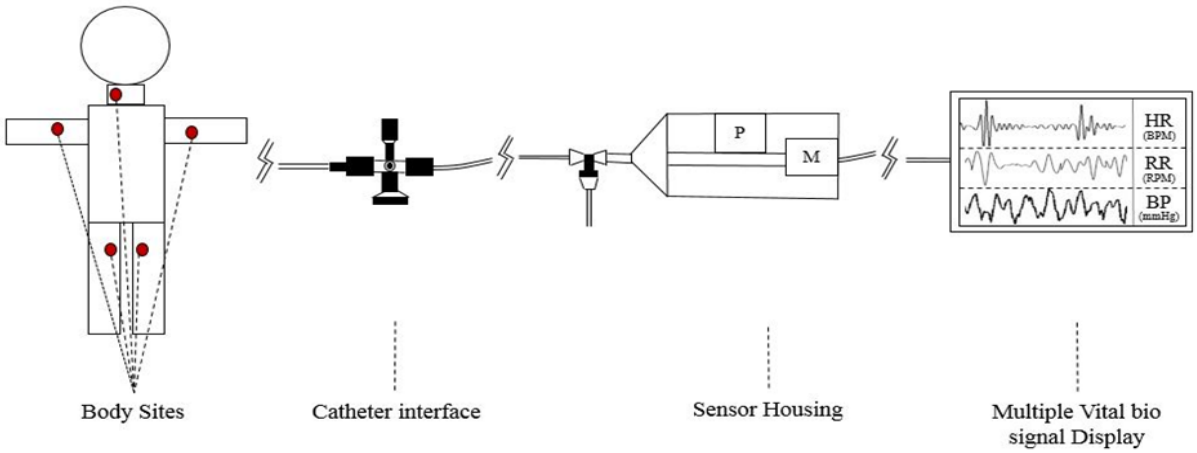

Figure 1.2: Critical and Emergency Care Monitoring Using Novel Catheter Multiscope.

parameters by uniquely characterizing a physiological process, i.e., blood flow dynamics. Figure 1.2 shows a basic overview of the concept of operations for the catheter multiscope monitoring critical parameters from a subject in critical and/or emergency care.

Figure 1.3 shows the life cycle representation of the medical device development. Following the lifecycle, proof of concept and feasibility studies will be carried out to evaluate the usability of the catheter multiscope for critical care using a small animal model [18]. The proposed novel catheter multiscope is an enhanced version of the electronic catheter stethoscope [19] with respect to its data acquisition. In particular, the limitations of the existing blood flow based data acquisition systems in detecting the sensitive variations within the dynamic pressure will be addressed through integration of the enhanced data acquisition system and an advanced signal processing framework. The proposed novel catheter multiscope is expected to be a disruption in technology, such that, it will be potentially possible to address open challenges such as the need for expensive instrumentation and complex infrastructure; improvement in the diagnostic precision in low resource settings; and functional interoperability. Further, the developed signal framework will also be extended to highlight the diagnostic potential of this technology for various case study applications. Specifically, proof of concept studies will be performed on applications such as sinus rhythm pattern recognition and fetal monitoring through phonocardiography. The proof of concept studies will demonstrate that the catheter multiscope can also be configured to be scalable and portable.

Figure 1.3: Medical Device Life Cycle.

1.4 Contributions

A novel critical and emergency care monitoring system has been developed to measure heart rate, respiratory rate, systolic and diastolic pressure with clinical accuracy from the blood flow dynamics.

- Designed an innovative data acquisition system to uniquely characterize the blood flow dynamics.
  - The data acquisition system was designed to precisely characterize the sensitive dynamic pressure variations of the blood flow using a fluid coupled catheter and a novel polymeric membrane to act as fluid to air coupler.
  - The data acquisition system was also designed to deliver the pressure field without any distortions while minimizing other interferences using a waveguide.
- Developed an innovative signal processing framework to extract vital bio-signals and the corresponding signal processing algorithms to compute critical parameters from the acquired blood flow dynamics.
  - Developed an efficient noise reduction algorithm to improve the signal to noise ratio of the acquired dynamic pressure field.
  - Developed a source separation algorithm to separate the data corresponding to various acoustic sources from a single channel observation.
  - Developed a validation metric to estimate the performance of denoising when the channel noise is not available.
- Developed a procedure to validate and benchmark the performance of the proposed critical and emergency care data acquisition system.

- Accomplished validation by comparing the critical parameters derived from the novel catheter multiscope to critical parameters derived from conventional measurement systems.

In addition to demonstrating the feasibility of the developed novel catheter multiscope in critical and emergency care monitoring, the diagnostic potential of the developed technology has been shown in the following case studies.

- Accurately recognized the sinus rhythm patterns using acoustic heart pulses from the novel catheter multiscope.
  - Developed a new feature called multiscale energy.
  - Developed a pattern recognition framework based on K-Means clustering.
- Extracted the vital bio-signals of fetal phonocardiograms with fidelity.
  - Implemented the catheter stethoscope's noise reduction and source separation framework to separate fetal and maternal heart sounds corresponding to various signal to noise ratio conditions of simulated fetal phonocardiograms
  - Validated the denoising and separation fidelity using validation metrics of the developed catheter multiscope.

In comparison to the existing state-of-the-art, the developed critical and emergency care monitoring technology exhibits innovation in terms of complexity of the data acquisition system and a signal processing framework. The proof of concept and the feasibility studies show that the developed minimally invasive catheter multiscope can be used to measure critical parameters with clinical accuracy. It is expected that this dissertation will serve the needs of scientists, researchers, clinicians and other readers involved in the research and development of medical devices and biomedical signal processing.

1.5 Dissertation Organization

The research that has been performed is organized and presented in the following chapters.

1.5.1 Chapter 2: Survey of Critical and Emergency Care Monitoring Systems

In this chapter, the background information about critical and emergency care monitoring and diagnostics is described. The diagnostic relevance of monitoring specific hemodynamic cardiovascular vital bio-signals in the critical and emergency care are also highlighted. A literature review on existing state-of-the-art critical care sensing technologies and clinical information systems is included in this chapter. In addition, a comprehensive introduction to various physiological signals (vital bio-signals) is presented from the perspective of the signal processing field.

1.5.2 Chapter 3: Data Collection

In this chapter, an overview of the human circulation system from the perspective of fluid mechanics and how various physiological systems influence the blood flow dynamics is provided. Then, how the data was collected for the feasibility study is described. Based on the fluid mechanics understanding of the human circulatory system, the interpretation of the collected data is provided. Finally, the chapter is concluded by laying the foundation for the development of the signal processing framework.

1.5.3 Chapter 4: Signal Processing Framework

In this chapter, a functional overview of the signal processing framework that was implemented to compute the vital bio-signals and critical parameters is provided. Further, a comprehensive description of the developed noise cancellation, the wavelet source separation and the novel blood pressure computation framework is presented. In addition, performance comparison results of various noise cancellation algorithms are provided. Finally, the chapter is

concluded by describing the validation results of wavelet source separation and blood pressure computation.

1.5.4 Chapter 5: Application Case Studies

In this chapter, an overview of special applications such as sinus rhythm pattern recognition and fetal monitoring through phonocardiography is provided. Further, a detailed description and results of feature extraction and pattern recognition framework for sinus rhythm pattern recognition are provided. Then, the chapter is concluded by providing the results of the noise cancellation and source separation techniques on the simulated fetal phonocardiograms.

1.5.5 Chapter 6: Conclusions and Future Research

A summary of the findings of this research is provided in this chapter. Then, directions for future research with respect to the data acquisition system design, data collection and signal processing framework have been provided in this chapter. In particular, the specifications and design for future generations of the data acquisition system is described. In addition, future directions for additional application case studies are also provided.

CHAPTER 2: REVIEW OF CRITICAL AND EMERGENCY CARE MONITORING PARAMETERS AND SYSTEMS

2.1 State-of-the-Art in Critical and Emergency Care Monitoring

Critical and/or emergency care begins with minimum standards of monitoring. However, depending on the status of the patient, a full spectrum of hemodynamic cardiovascular parameters come into play that aid in determining the future clinical interventions. The complete set of critical parameters can be classified into four groups. They are pressure, cardiovascular, respiratory and miscellaneous. In addition to the parameters, their respective sensing technologies are also shown in Table 2.1. In addition to the traditional sensing technologies, a number of other alternative technologies are often employed to estimate other critical hemodynamic and respiratory parameters. This chapter provides an introduction to the morphology of all the vital bio-signals, an overview of all the fundamental hemodynamic parameters, a review of the existing sensing technologies, clinical information systems and other frequently used alternative technologies.

Table 2.1: Critical and Emergency Care Cardiovascular Hemodynamic Parameters.

Cardiovascular Parameters	**Sensing Technology**
Heart Rate (HR)	ECG, PCG, Pulseoximetry, Blood Pressure
Cardiac Output (CO)	Dilution Methods, Pulse Wave Velocity Analysis and Bioimpedance
Pressure Parameters	**Sensing Technology**
Mean Arterial Pressure (MAP)	Arterial Catheter
Central Venous Pressure (CVP)	Central Venous Catheter
Mean Pulmonary Arterial Pressure (MPAP)	Pulmonary Arterial Catheter
Pulmonary Arterial Occlusion Pressure (PAOP)	Pulmonary Arterial Catheter

Table 2.1 (Contd.)

Respiratory Parameters	Sensing Technology
Respiratory Rate (RR)	Capnogram, Pneumatograph and ECG.
End Tidal Carbon-dioxide Pressure ($ETCO_2$)	Capnogram
Miscellaneous Parameters	**Sensing Technology**
Peripheral Oxygen Saturation (SPO_2)	Pulseoximetry
Arterial Hemoglobin Saturation (SAO_2)	Blood Sampling Analysis and Pulseoximetry
Arterial Oxygen Tension (PAO_2)	Blood Sampling Analysis
Mixed Venous Oxygen Saturation (SVO_2)	Blood Sampling Analysis
Mixed Venous Oxygen Tension (PVO_2)	Blood Sampling Analysis
Arterial pH (pH)	Blood Sampling Analysis
Hemoglobin (Hgb)	Blood Sampling Analysis
Core Temperature (T)	Pulmonary Arterial Catheter and Foley Catheter

2.1.1 Electrocardiogram (ECG)

ECG is a graphical representation of the electrical activity of the cardiovascular system. The wave-like pumping action of the heart is controlled by a network of neural fibers that are distributed throughout the myocardium and coordinate its regular contraction and relaxation. The myocardial stimulation starts from the Sinoatrial Node (SA-node). The SA-node is a cluster of cells located in the upper-right posterior wall of the right atrium, which sends the electrical impulse that triggers each heartbeat. This impulse further stimulates the second cluster of cells, namely the Atrioventricular Node (AV-node) that is situated in the lower posterior wall of the right atrium. After the AV-node, the depolarization front enters the bundle of His, the left and right bundles, and ends in the Purkinje fibers, depolarizing the ventricular muscles in its way. The procedure of myocardium contraction is known as the depolarization (or systole) cycle that is followed by the repolarization (or diastole) cycle, in which the myocardium relaxes and becomes ready for the next activation. A complete cardiac cycle is depicted in Figure 2.1. This cardiovascular electrical activity is transmitted throughout the body and can be measured across the chest using either 1-

lead or 3-lead or 5-lead or 6-lead or 12-lead skin electrodes. For critical and emergency care, 12-lead ECG is considered the gold standard, due to its measurement accuracy [20].

The ECG measured on the body surface is a result of the stage-wise activation of the myocardium and results in the PQRST-complex depicted in Figure 2.1. The P-wave is the result of the atrial depolarization. This depolarization starts at the SA-node and spreads to ventricles through the AV-node. The QRS complex represents the ventricular depolarization. Then, atria and ventricles repolarize. However, atrial repolarization is obscured by the QRS complex and ventricle repolarization is represented through the T wave [21]. One of the main uses of ECG in the critical and emergency care is continuous monitoring of heart rate. The heart rate represents the time consumed by the heart to complete one cardiac cycle. The HR is one of the high priority critical parameters and is typically measured as the time interval between current and previous R-waves of ECG. Arrhythmias are other leading cause of death among critical and emergency care patients. Hence, many critical and emergency care units detect arrhythmia through continuous ECG monitoring. In addition, ECG is also used to provide complimentary information about respiratory system through RR computation [22]. Though ECG provides significant diagnostic information, its use is limited due to some critical challenges. ECG data acquisition is complex and due to this, it is known to induce discomfort and restrict patient mobility. Studies like [23] [24] have often shown that morphological characteristics of the ECG change due to electrolyte, water and other chemical changes in the cardiovascular system. In the context of critical and emergency care, drugs, medication and nutrients are frequently delivered to induce changes in the micro and macro circulation. This often leads to changes in the cardiovascular system's electrolyte composition. This composition change will result in diagnostic errors and false alarms due to the changes in the ECG's morphological characteristics. Hence, there is an increased need to develop a medical

device that provides reliable and consistent results even during chemical composition change in the cardiovascular system and that addresses other ECG limitations. In addition to the ECG, an alternative technology that records acoustic activity of the heart is often used. This is known as phonocardiogram and it provides vital information with respect to cardiovascular abnormalities [13].

2.1.2 Blood Pressure (BP)

High blood pressure is a leading risk factor responsible for high cardiovascular morbidity and mortality rates. Hence, precise and accurate monitoring of continuous blood pressure is imperative in critical and emergency care. The main function of the human circulatory system is to transport oxygen and other nutrients to the tissues and to carry waste away from the cells. The nutrients and the oxygen are carried to various parts of the body through oxygenated blood flow via arteries, and waste through deoxygenated blood flow via veins. The blood flows in the blood vessels due to the pumping action of the heart. The heart can be divided into four chambers and two pumping systems. Each pump has a filling chamber known as the atrium, which helps to fill a pumping chamber known as the ventricle. The oxygenated blood flows from the lungs into the left ventricle through left atrium and mitral valve. The left ventricle then ejects the blood into the aorta through the aortic value. Blood is then distributed to various parts of the body through branching network of arteries, arterioles and ventricles. Similar to the arterial system, the deoxygenated blood from different parts of the body reaches the right atrium through the venous system. The deoxygenated blood flows into the right ventricles through the tricuspid valve and into the pulmonary artery through the pulmonary valve. During diastole, the atria contract to generate sufficient pressure to open the mitral and tricuspid valves, thereby filling the ventricles. Then, during systole, aortic and pulmonary valves open due to pressure generated by ventricular

contraction. This mechanical contraction of the ventricles forces the blood to flow in arteries and veins [8]. In effect, the flowing blood exerts pressure onto the walls of the blood vessels contributing to blood pressure.

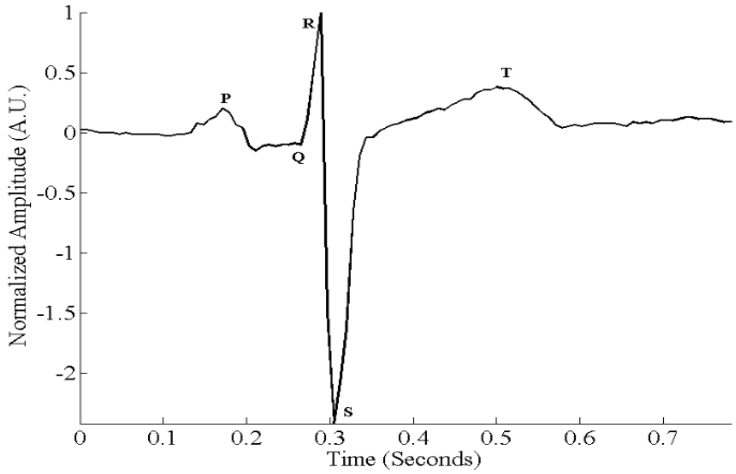

Figure 2.1: Morphology of the Electrocardiogram. Data Obtained from MIT–BIH Long-Term ECG Database [25].

Many technologies exist to measure blood pressure. They can be classified into three groups based on the measurement technique: invasive, oscillometric and unobtrusive, also known as cuffless. In the context of critical and emergency care, since continuous monitoring of the blood pressure is imperative, invasive blood pressure measurement is considered to be the gold standard. Invasive blood pressure measurement typically involves the use of a catheter. Based on the location of the sensing element, invasive measurement can be further classified into intravascular and extravascular measurement systems. In the extravascular pressure measurement systems, the vascular pressure is fluid coupled to an external sensing element. The catheter is inserted into the arterial or venous system through a cannula, where the proximal end of the cannula is immersed in the blood and the distal end is connected to the proximal end of the fluid filled catheter. The distal end of the fluid filled tube is connected to either a drug delivery system or a saline delivery

system. The column that couples the vascular pressure through fluid to the diaphragm of the pressure transducer is housed before the drug delivery system as shown in Figure 2.2.

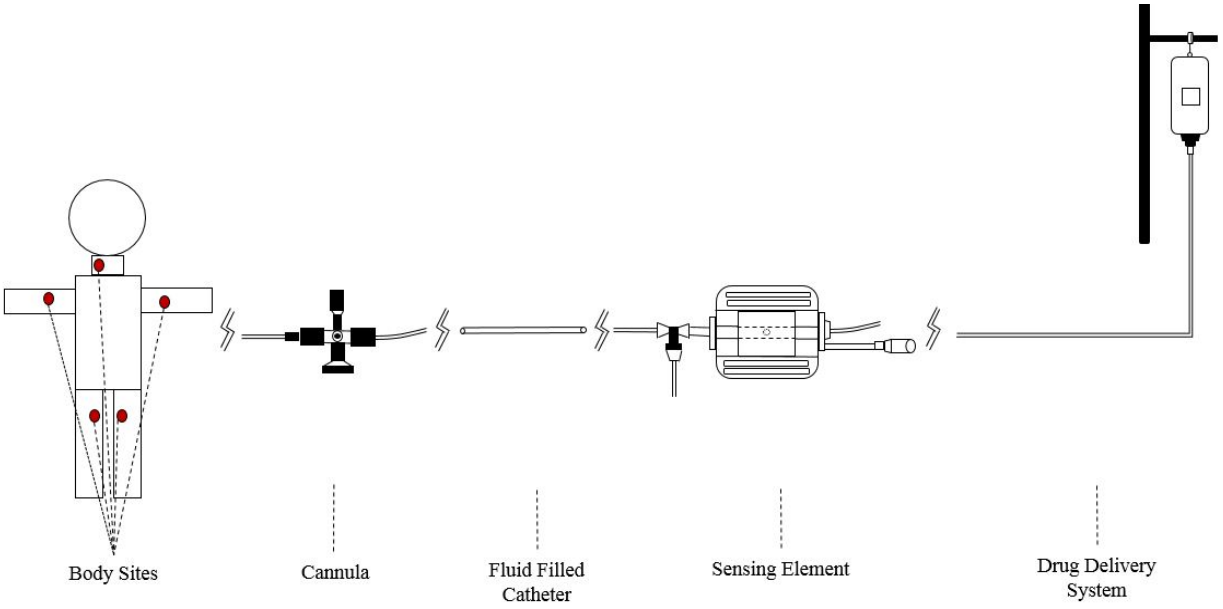

Figure 2.2: Invasive Extravascular Pressure Measurement System.

On the other hand, in the intravascular pressure measurement systems, the sensing element is housed at the tip of the catheter and is placed directly into the vascular system. Among non-invasive blood pressure measurement techniques, the oscillometric technique is a widely used method. The oscillometric techniques estimate the blood pressure through auditory detection of the turbulent blood flow sounds occurring due to inflation of the occlusive cuff around an artery. These turbulent blood flow sounds are detected using a stethoscope by stepwise deflation of the inflated cuff. The pressure detected at the first and the last instances of the turbulent blood flow sounds are considered to represent pressure during systole and diastole, respectively. Unobtrusive blood pressure monitoring methods are among recent developments and are still under research. The objective of unobtrusive monitoring is to estimate blood pressure continuously and non-invasively. Existing unobtrusive methods estimate blood pressure by linearly or nonlinearly modeling the pulse transit time or the pulse wave velocity. Pulse transit time or pulse wave velocity

is currently being measured using either electrical, optical, magnetic, mechanical or impedance based sensing technologies [8] [26] [27].

It is worth noting that the blood pressure is different at various body sites. In particular, arterial pressure, central venous pressure and pulmonary arterial pressure are the most widely monitored vital bio-signals in critical and emergency care. Arterial pressure is representative of pressure of blood exerted on the walls of arteries. This pressure is commonly measured in radial, femoral, carotid arteries or aorta through the use of an arterial catheter. The arterial pulse is a forward propagating pressure wave that is generated due to stroke volume changes during each cardiac cycle. The arterial pressure waveform is a periodic waveform that can be represented as a summation of six sinusoidal components. Each local maxima in the waveform occurs when the ventricle contracts and forces the blood into the aorta, this is referred to as systolic pressure. Similarly, local minima in the waveform occur after the aortic valve closes and when the ventricles relax; this is referred to as diastolic pressure. In addition, the arterial pressure waveform also reflects the valve closure as a high frequency interruption in the signal and it is commonly referred to as the dicrotic notch. As the pressure reaches the minima, the aortic valve opens and the blood starts flowing into the aorta, usually seen as an increasing signal with positive slope and the pressure reaches a local maxima. This process periodically repeats for each cardiac cycle [28]. From the arterial blood pressure vital bio-signal, critical parameters such as systolic, diastolic and mean arterial pressures are estimated. The critical parameters estimated from arterial blood pressure vital bio-signal contain information with respect to afterload, i.e., tension developed by the myocardium during ventricular systolic ejection [5] [29]. In addition to the after load, information with respect to preload is also another parameter that is measured in critical and emergency care. Preload provides information with respect to intravascular volume, i.e., amount

of blood returned to the heart which is reflective of perfusion abnormalities. This is accomplished by measuring CVP, i.e. pressure in the right atrium, using a central venous catheter. The CVP waveform is typically represented by acxvy components. Each component of the CVP waveform has a direct relevance to the events of a cardiac cycle [30]. Pulmonary arterial pressure is another vital bio-signal that is continuously monitored for high risk patients in critical and emergency care. The pulmonary arterial pressure is measured using a balloon tipped Swan-Ganz catheter. The Swan-Ganz catheter is typically placed in pulmonary artery and the pressure is recorded. In addition, when the balloon tip of the catheter is inflated and placed in a branch of the pulmonary artery, the measurement results in the PAOP. The waveforms of the pulmonary arterial pressure and the PAOP are also characterized by the a, the c and the v components. MPAP and mean PAOP (MPAOP) are the critical parameters that are computed from pulmonary arterial pressure signals [31] [32]. In addition to pulmonary arterial catheter, recent developments have led to the assessment of MPAP and MPAOP using ultrasound technology [33] [34] [35]. Figure 2.3 shows various waveforms collected as of part of intensive care monitoring in The Massachusetts General Hospital and published as "The MGH/MF Waveform Database" in the PhysioNet databank [36] [25].

Various technologies exist to assess the pressure based vital bio-signals and the corresponding critical parameters. In the context of critical care, catheter based pressure measurements are considered to be gold standard to date. However, these catheter based pressure measurement systems provide limited information. As of today, these systems only provide blood pressure information. However, in order to get information with respect to other fundamental critical parameters, today's standard of care has to rely on other technologies. With few

modifications, the catheter based systems will be able to provide all the fundamental critical parameters. This is one of the main challenge that is addressed in this dissertation.

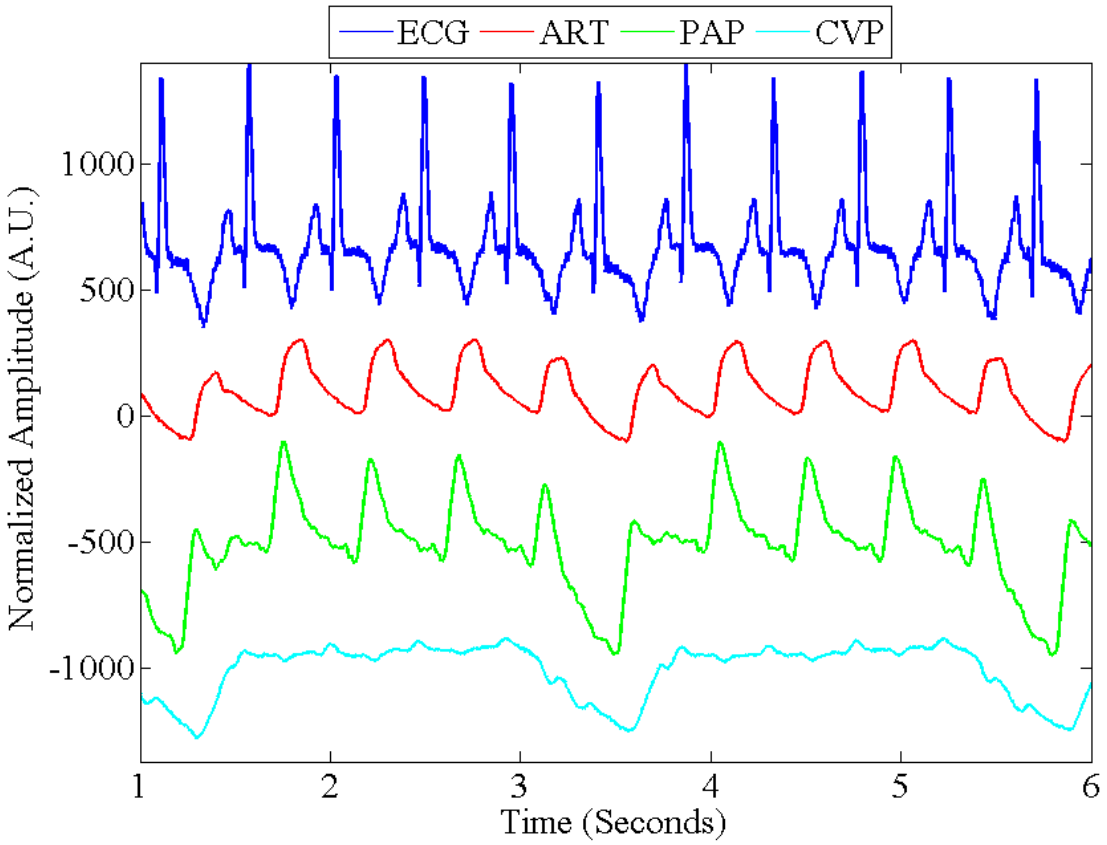

Figure 2.3: Morphology of ECG, ART, PAP, CVP Bio-signals. Data Obtained from [36] [25].

2.1.3 Cardiac Output (CO)

Cardiac output is one of the most important critical parameters that is continuously monitored for high risk patients in critical and emergency care. It is defined as the volume of blood pumped by the heart per minute. CO is a widely used diagnostic tool to detect various conditions including cardiovascular shocks and also to determine if fluid resuscitation and other medications are needed based on the hemodynamic profile. Traditionally in critical and emergency care, CO is measured using a pulmonary arterial catheter and a dilution technique. In the dilution techniques, an agent of known concentration and temperature is injected into the right atrium through the distal

end of the pulmonary arterial catheter. Due to constant stroke volume change, the concentration of the mixture of agent and blood starts reducing and the temperature of the blood changes. This change in the temperature of the blood is monitored constantly as the thermodilution curve. The measured temperature and the initial volume of the agent in combination will be used to determine the CO [37]. CO can also be estimated using ultrasound and echocardiography, in particular, the distance traveled by a column of blood for each cardiac cycle is estimated, i.e., blood flow velocity. The measured blood flow velocity is directly proportional to stroke volume and hence CO. CO can also be estimated using technologies that involve bioimpedance and pulse contour analysis techniques. In the bioimpedance method, the change in the impedance of the electrodes placed on the chest is directly correlated to the blood volume change used to estimate the CO. On the other hand, the pressure pulse velocity is determined using either electrical, optical, magnetic, mechanical or impedance based sensing technologies which can be linearly or nonlinearly modeled to estimate CO. Based on the techniques discussed, various alternative sensing technologies have been developed to provide information with respect to CO as described in [38] [39].

2.1.4 Capnography

Continuous monitoring of the cardiorespiratory system is essential to provide necessary ventilation support for patients in critical and emergency care. Although, different parameters provide relevant information with respect to the respiratory system, RR and $ETCO_2$ are the essential critical parameters being used today. They are typically derived from the capnogram, a vital bio-signal. Capnography is a method used to detect the concentration of carbon-dioxide in a sample of gas. The sample of gas exchanged by the patient is collected either through a nasal cannula or through an intubation tube for absorption spectroscopic analysis. As the carbon-dioxide absorbs the infrared light, the transmitted spectra is analyzed and calibrated to provide the

concentration of carbon-dioxide in the subject's gas sample. Measuring and tracing this carbon-dioxide concentration over time will result in the vital bio-signal called capnogram. The capnogram is a periodic waveform that represents events of a complete respiratory cycle. The events of respiratory cycle are inspiration, expiratory stroke, expiratory plateau and expiratory downstroke. During inspiration, the concentration of the carbon dioxide remains to be at a consistent baseline line, then as the expiratory begins, the alveolar gases get emitted. The alveolar gases predominantly contain carbon dioxide and hence its concentration begins to reach a local maxima, i.e., gets plateaued. After the complete volume of alveolar gases get expired, the inspiration begins. Right after inspiration, and before expiratory plateau, there is a momentary dead space when the both the inspiratory and alveolar gas exchange ends, this region is known as expiratory stroke. Also, as soon as the concentration of carbon dioxide reaches a local maxima, there exists some dead space when both the expired and inspired gas exchange end, this is known as the expiratory downstroke. From this waveform, critical parameters, RR and $ETCO_2$ are computed. RR is computed as time expired for both inspiration and expiration per minute; $ETCO_2$ is the maximum concentration of the CO_2 in the expired gas i.e., the local maxima of the event expiratory plateau. In addition to time-based capnogram, volume based capnogram is also widely used. Additional details on capnography based cardiorespiratory monitoring and trends in capnography technologies are presented in [40] [41] [42]. In addition, volume based critical parameters such as tidal volume, vital and total lung capacities are measured using spirometers, pneumatographs and other alternative technologies [43].

2.1.5 Plethysmograph

Ensuring oxygen delivery to tissues is one of the main objectives of the cardiorespiratory system. During respiration, the inspired oxygen in the lungs bind to deoxygenated blood, making

it oxygenated blood. Most of the oxygen in the lungs bind to hemoglobin. Small amount of oxygen dissolves in the blood plasma. This oxygenated blood is then pumped out of the heart into the aorta, and then into the arteries, arterioles and eventually into the capillary networks. These networks of capillaries supply tissues with oxygen and nutrients. Plethysmograph is a tracing of the amount of oxygen that is bound to hemoglobin at the tissue level, also known as SPO_2. The oxygenated and deoxygenated hemoglobin levels in the blood are detected using absorption based infrared spectroscopy transcutaneously. The vital bio-signal waveform obtained using spectroscopy is known as plethysmography or pulse oximetry. This waveform contains information with respect to arterial blood, tissue, and respiration. It contains an AC and a DC component. The percentage of SPO_2 is the critical parameter that is calculated using amplitude ratios of both the AC and the DC components of plethysmography. It has to be noted that, SPO_2 is considered to be an indirect measurement of SAO_2. Additional details of the plethysmography are described in [44] [45].

2.1.6 Miscellaneous Critical Parameters

Arterial hemoglobin saturation (SAO_2), arterial oxygen tension (PAO_2), mixed venous oxygen saturation (SVO_2), mixed venous oxygen tension (PVO_2), arterial pH (pH), hemoglobin (Hgb) and core temperature (T) are among the other miscellaneous critical parameters that are often measured in critical and emergency care. SAO_2 is the measurement of concentration of oxygenized hemoglobin in the arterial blood and PAO_2 is the measurement of concentration of the oxygen dissolved in arterial blood plasma. In addition to critical parameters corresponding to the arterial blood, parameters corresponding to venous oxygenation such as SVO_2 and PVO_2 are also measured. SVO_2 is the measurement of oxygen concentration bound to hemoglobin in venous blood, and PVO_2 is the measurement of oxygen concentration dissolved in venous blood plasma.

These parameters are measured using either blood sampling analysis or by using an indwelling fiber optic catheter. In blood sampling analysis, a column of blood is sampled from either an arterial or a venous body site and is subjected to spectroscopic analysis using blood gas analyzers. In order to measure the concentration of the blood plasma in arterial or venous blood, the blood cells are separated from blood plasma either using centrifugal techniques or using a reagent. Then, the plasma is made to interact with a metal testing strip to determine the concentration of compounds of interest in the plasma. In addition, various alternative techniques involving spectroscopy systems in combination with linear and nonlinear modeling are being developed for rapid blood analysis. It also has to be noted that, other parameters such as total hemoglobin, concentration of other electrolytes and acidity level within the blood are monitored for patients with advanced risk in critical and emergency care. Core temperature is also a parameter that is usually measured from a sample extracted from either pulmonary arterial catheter or urinary Foley catheter. Additional information regarding miscellaneous parameters and electrolyte concentration is provided in [46] [47] [48] [49].

2.1.7 Clinical Information Systems

It is well established that there are several vital bio-signals corresponding to various physiological processes that must be continuously monitored in critical and emergency care. In addition, various critical parameters corresponding to the vital bio-signals are also continuously computed and monitored. A clinical information system is often employed in critical and emergency care to integrate and visualize the critical parameters and vital bio-signal collected from corresponding physiological processes. As of today, several clinical information systems are commercially available to provide end-to-end solutions to integrate diverse patient sensing or monitoring systems. It is estimated that the market value for these system has exceeded $1.3 billion

due to the volume of information available in the intensive and emergency care setting. Currently, GE's Centricity and Philips IntelliVue Clinical Information Portfolio are the most commonly used commercial critical and emergency care information systems [17]. The vital bio-signals corresponding to various physiological processes are typically generated by standalone sensing technologies and either analog or digital data is available depending on the technology. The data available from these technologies is integrated through either a serial (RS-232 or I2C or USB), Ethernet (802.3) port or using wireless (802.11b/g or Bluetooth) communication for digital data. For analog data, standard hardware interfaces are used. Though, high resolution physiological data is not collected, snapshots of the acquired vital bio-signals and critical parameters are displayed on monitors to aid in the clinical decision making. In addition, a standard architecture to integrate and acquire continuous physiological data is yet to be established. Recent developments in clinical information systems can be found in [17].

CHAPTER 3: DATA COLLECTION

3.1 Fluid Mechanical Perspective of Blood Circulation

The circulatory system can be described as a closed loop system that is directly regulated by the cardiovascular system and the respiratory system and controlled by the nervous system. As a result, the dynamics of the blood flow is influenced by factors such as length of cardiac cycle, stroke volume, rate of respiration, volume of respiration and baroreflex control. This complex interrelationship within various subsystems of the human body make the dynamics of the blood flow an interesting phenomenon. Several studies in the literature have underlined the significance of various factors that affect the blood flow, Cardiac Output (CO), i.e., the amount of blood pumped by the heart per minute, which is usually computed as a product of HR and stroke volume. Thus, increasing the heart rate or increasing the contractile strength of the ventricles, i.e., stroke volume, CO can be increased. In addition, it is well established that variability of heart rate is influenced by the baroreflex control and the breathing in the form of Meyer waves and respiratory sinus arrhythmia [50] [51]. In addition to CO, blood flow dynamics is also affected due to the properties of the arteries and veins. The properties of the arteries and veins such as elasticity, vascular resistance and thus the diameter of the corresponding blood vessels are controlled by the baroreflex feedback [52] [53]. Studies have also shown that baroreflex controls the dynamics of the blood flow based on the respiratory parameters such as volume and rate of respiration [54] [55] [56] [57] [58].

The circulatory system can be approximated as a fluid pumping system as shown in Figure 3.1. In Figure 3.1, the deoxygenated blood is collected from the organs and is sent to the lungs. Then, the oxygenated blood is collected from the lungs and is distributed to the organs. According to Bernoulli's principle, the total energy of any frictionless fluid flow is conserved. As a result, blood flow in the blood vessels can be described using Bernoulli's principle. The total energy of the blood flow in any blood vessel is the summation of its static pressure, dynamic pressure and gravitational head. The static pressure of the fluid is the pressure generated due to the force exerted by all the fluid elements on each other i.e. intramolecular pressure. In the case of steady state flow, the static pressure is directly dependent on the volumetric flow rate of the fluid. Due to this static pressure, the blood exerts pressure in all directions including on the walls of the blood vessels, contributing to blood pressure. In addition, since the blood is pumped with some velocity by the ventricular contraction during each cardiac cycle, the fluid also contains kinetic energy that is directly proportional to its velocity. This kinetic energy is often referred to as dynamic pressure. In addition, the pulsatile flow of blood influences the flow within the blood vessels with an unsteady acceleration. Overall, the pressure wave propagates mainly due to radial and axial fluid motion. While radial motion is due to the static pressure, axial motion is due to the dynamic pressure [8] [59]. Also, since the pressures are acquired at an increased elevation, the fluid also exhibits gravitational head due to the weight of the fluid. As of to date, blood flow has been mainly used to obtain information with respect to blood pressure. However, since the blood flow dynamics contain a plethora of information in the form of multi-dimensional pressure wave with regards to various cardiovascular, respiratory, and other subsystems, the blood flow dynamics was selected as a phenomenon of interest to obtain multiple critical parameters. In this dissertation, a novel data acquisition system was designed to characterize the blood flow dynamics and to obtain information

with respect to multi-dimensional pressure field. The details of the design and the data collection are provided in the following sections[1,2].

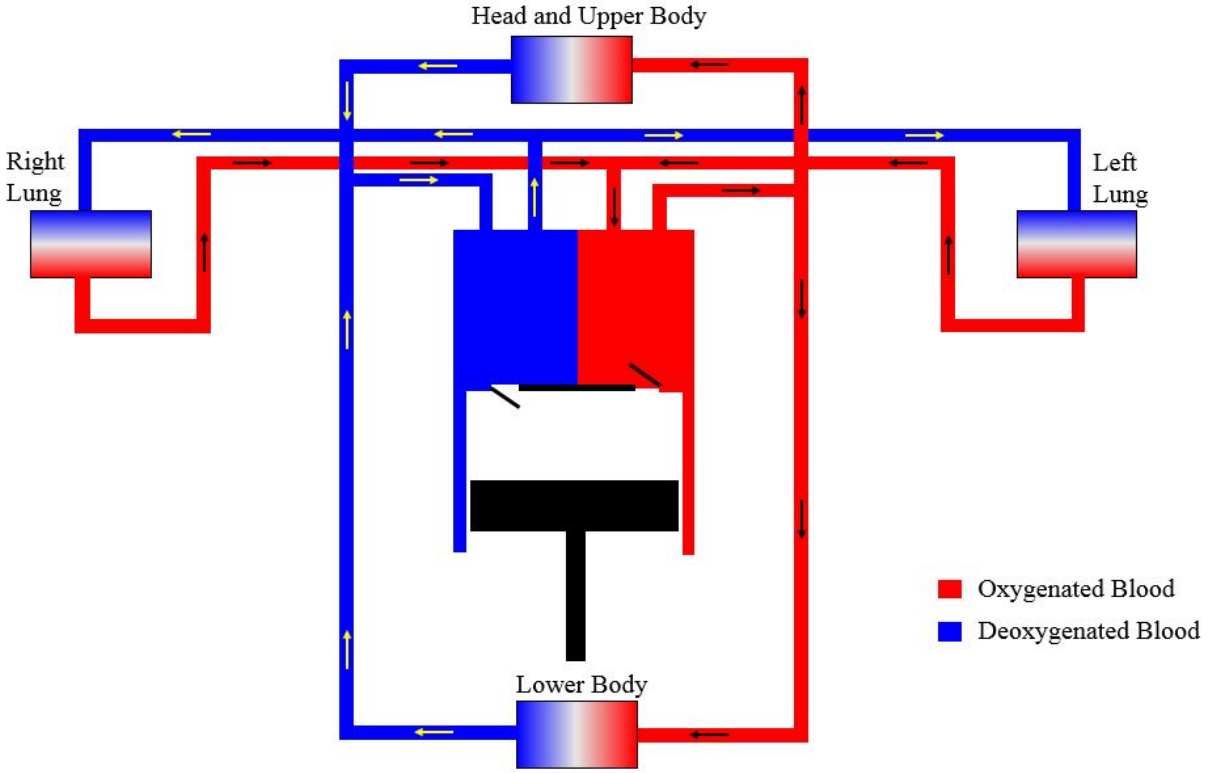

Figure 3.1: Fluid Pumping System Approximation of Circulatory System.

3.2 Data Acquisition System Design

Figure 3.2 illustrates the block diagram overview of the data acquisition system that was used to determine multiple vital bio-signals from the animal model. As shown in Figure 3.2, the system includes a silicone or polyvinylchloride catheter comprising a flexible tube that is configured for insertion in a subject's blood vessel, such as an artery or vein. When inserted, the distal end of the catheter is immersed in the blood that flows through the vessel. The proximal end of the catheter is received by, and therefore connected to, a coupling member that is, in turn, connected to a waveguide. As is also shown in Figure 3.2, a port has been provided along the

[1]The content described in Chapters 3 and 4 are part of US provisional [122] and utility patent applications [123].
[2]A preliminary version of the content presented in Chapter 3 and 4 have been published in the proceedings of 39th annual international conference of the IEEE Engineering in Medicine and Biology Society [121].

length of the catheter between its distal and proximal ends that can be used to flush the catheter with an appropriate fluid, such as saline solution. Mounted to the coupling member is a flexible barrier. This barrier is formed using a thin polymeric membrane that is on a first side in fluid communication with the blood delivered to the coupling member by the catheter and on a second side in fluid communication with air contained within an interior air chamber of the waveguide. At the proximal end of the waveguide, a pressure field microphone isolated from the environment is housed to measure the pressure within the waveguide. The waveguide that is housing the pressure field microphone is mounted on a vibration isolating stainless steel tray. In addition, a free field microphone placed within close proximity to the subject is also used to measure reference acoustic noise. Specifically, the free field microphone is directed towards the subject using a stainless steel holder mounted on a tripod. It also has to be noted that both pressure and free field microphones were located at the same elevation from the ground as that of the subject and forming an angle less than 45^{o} among themselves during the measurement. In the current feasibility study, a GRAS 46 AD, a pressure field microphone with frequency response of 3.15 Hz – 10 kHz and a G.R.A.S 46 AE, a free field microphone, have been used to measure pressure field and reference acoustic noise respectively [60] [61]. Since both G.R.A.S microphones require a constant current power supply of 4 mA and 24 V for optimal performance, a National Instruments PXI 4462 system is used to provide constant power to the microphones through a British naval connector. The measured data from both the channels was digitized and stored at a sampling frequency of 10 kHz and 24 bit quantization rate using PXI 4462 system and LabVIEW data acquisition drivers [62]. As shown in Figure 3.2, the waveguide is designed to be conical and special attention has been paid to estimate the ideal distance between the barrier and the microphone based on the length of the sensing element. These design considerations have enabled maximal energy transfer while

attenuating the effects of reflections and reverberation and without distorting the frequency of the actual pressure wave.

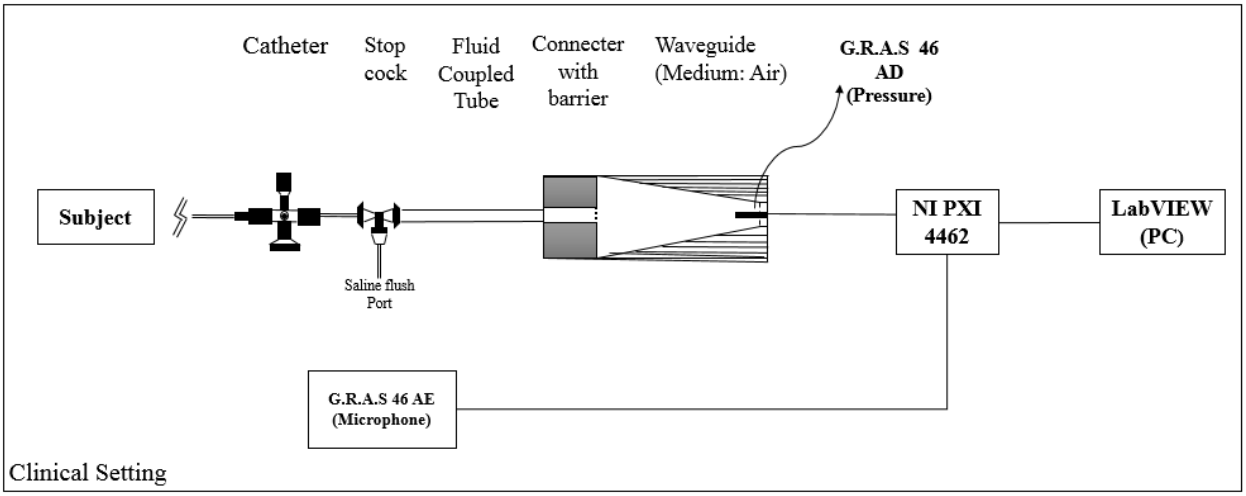

Figure 3.2: Block Diagram Representation of the Data Acquisition System.

3.3 Data Collection Approach

The data collection approach defines type and location of the data being acquired. Vascular pressures were obtained from various arterial and venous body sites of an anesthetized Yorkshire pig in supine position. The obtained vascular pressures were coupled from the subject to the extravascular pressure field microphone through a fluid coupled catheter using a preexisting arterial or venous line. A total of twelve pressure measurements were obtained from six different body sites as part of this study. Two different pressure measurements were obtained at each body site, one without the influence of epinephrine and other with influence of epinephrine. Table 3.1 illustrates the sequence in which the design of experiments was conducted for all the acquired pressure measurements. In addition, heart rate, respiratory rate and blood pressure were measured prior to and post the vascular pressure acquisition for the purpose of benchmarking. These parameters were obtained from the state-of-the-art Philips IntelliVue critical care clinical information system. It has to be noted that, this study was performed by strictly adhering to ethical standards of the Institutional Animal Care & Use Committee. In addition, all the animal studies

corresponding to this research were performed at the University of South Florida's Center for Advanced Medical Learning and Simulation facilities eCath laboratory. Appendix B contains relevant documentation with regards to IACUC approval for the animal studies.

Table 3.1: Design of Experiments For Measured Blood Flow Dynamics.

Recording Index	**Body Site**			**Catheter Size**	**Epinephrine**
1a	Artery	Carotid	Left Side of Neck	5F	No
1b	Artery	Carotid	Left Side of Neck	5F	Yes
2a	Venous	Jugular	Right Side of Neck	5F	Yes
2b	Venous	Jugular	Right Side of Neck	5F	No
3a	Venous	Femoral	Right Leg	4F	No
3b	Venous	Femoral	Right Leg	4F	Yes
4a	Venous	Femoral	Left Leg	6F	Yes
4b	Venous	Femoral	Left Leg	6F	No
5a	Artery	Peripheral	Left Ear	20F	No
5b	Artery	Peripheral	Left Ear	20F	Yes
6a	Artery	Femoral	Left Leg	5F	No
6b	Artery	Femoral	Left Leg	5F	Yes

3.4 Description of the Measurements

The blood flows from the venous or arterial body site into the catheter and reaches the flexible barrier that stagnates the flow of blood and ultimately acts as a fluid to air coupler. At this boundary, the blood column oscillates and this oscillation depends on the frequency of stagnation pressure of the blood flow, i.e., the frequency at which the blood is being pumped. The stagnation pressure that is impinged onto the barrier induces a pressure field in the waveguide. According to the basic principles of fluid mechanics, the total pressure (P_{total}) is the sum of static pressure (P_{static}) and dynamic pressure ($P_{dynamic}$) [63]. P_{static} results from intramolecular interaction and $P_{dynamic}$ results from the velocity of the blood flow. These pressures are traditionally measured using a combination of piezometer and Pitot tube. Based on the configuration in which the pressure field microphone was arranged to acquire pressure data, it was considered that the measured pressure is P_{total}. In order to understand how the stagnation pressure or total pressure is being measured,

Bernoulli's equations are used in the following derivation as means to provide a theoretical understanding of the measurements. Figure 3.3 presents a zoomed in view of the data acquisition system that was used is measuring P_{total} of the blood flow.

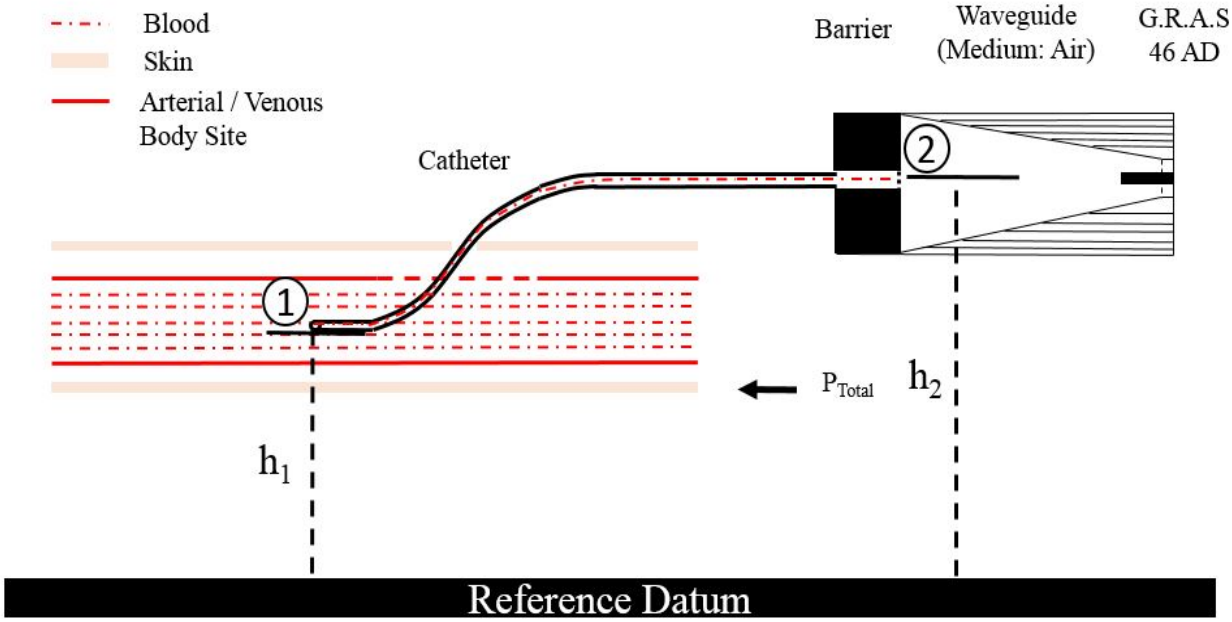

Figure 3.3: Zoomed in View of the Data Acquisition System.

As shown in Figure 3.3, the catheter orifice is at point 1, where point 1 is located at an elevation level h_1 from the reference datum and the barrier, i.e., the stagnation point 2 is located at an elevation level h_2 from the reference datum. In order to show that, the stagnation point 2 experiences P_{total}, the Bernoulli's energy conservation equations are written for points 1 and 2. Noting that at point 1, the static pressure is P_1 and the velocity is V_1 and at point 2, the static pressure is P_2 and the velocity is V_2. The following expression can be written using the Bernoulli's principle.

$$P_1 + \frac{1}{2}\rho V_1^2 + \rho g h_1 = P_2 + \frac{1}{2}\rho V_2^2 + \rho g h_2 \quad (1)$$

In equation (1), $\frac{1}{2}\rho V_1^2$ and $\frac{1}{2}\rho V_2^2$ are the dynamic pressures, $\rho g h_1$ and $\rho g h_2$ are gravitational heads at points 1 and 2, respectively. As the blood reaches the barrier, its velocity V_2 at point 2 becomes zero, resulting in the equations (2) and (3).

$$P_1 + \frac{1}{2}\rho V_1^2 + \rho g h_1 = P_2 + \rho g h_2 \quad (2)$$

$$P_1 + \frac{1}{2}\rho V_1^2 + \rho g (h_1 - h_2) = P_2 \quad (3)$$

Equation (3) proves that the barrier induces a pressure field equivalent to P_{total} into the waveguide. It was also observed that the pressure field microphone partly cancelled out the P_{static} data from the acquired P_{total} data through a static pressure equalization vent that was originally designed to equalize the effect of ambient pressure [64] [65]. Therefore, it was concluded that the acquired P_{total} predominantly consisted of pressure data corresponding to $P_{dynamic}$ and trace amounts of P_{static}. This provided motivation to derive the P_{static} from the acquired P_{total}. In standard invasive pressure measurement systems, P_{static} is the measured pressure and P_{total} is not measured. However, in this study, both $P_{dynamic}$ and P_{static} were measured by uniquely characterizing the acquired P_{total} as described in the next chapter.

CHAPTER 4: SIGNAL PROCESSING FRAMEWORK

4.1 Background of Processing Blood Flow Dynamics

The signal processing framework shown in Figure 4.1, follows a basic approach in the extraction and analysis of P_{static} and $P_{dynamic}$ from the measured P_{total}. Analyzing the acoustic field using the $P_{dynamic}$ processing framework resulted in the acoustic heart and respiratory pulses. Reconstructing the pressure field using the P_{static} processing framework resulted in the extraction of continuous blood pressure, i.e., systolic and diastolic pressures. P_{static} will be referred to as the pressure field and $P_{dynamic}$ as the acoustic field of the blood flow in the rest of this dissertation. As shown in Figure 4.1, the acoustic field was processed using noise reduction and source separation algorithms and the pressure field was processed using a novel compression and a sensor attenuation factor regression model to result in the corresponding vital bio-signals.

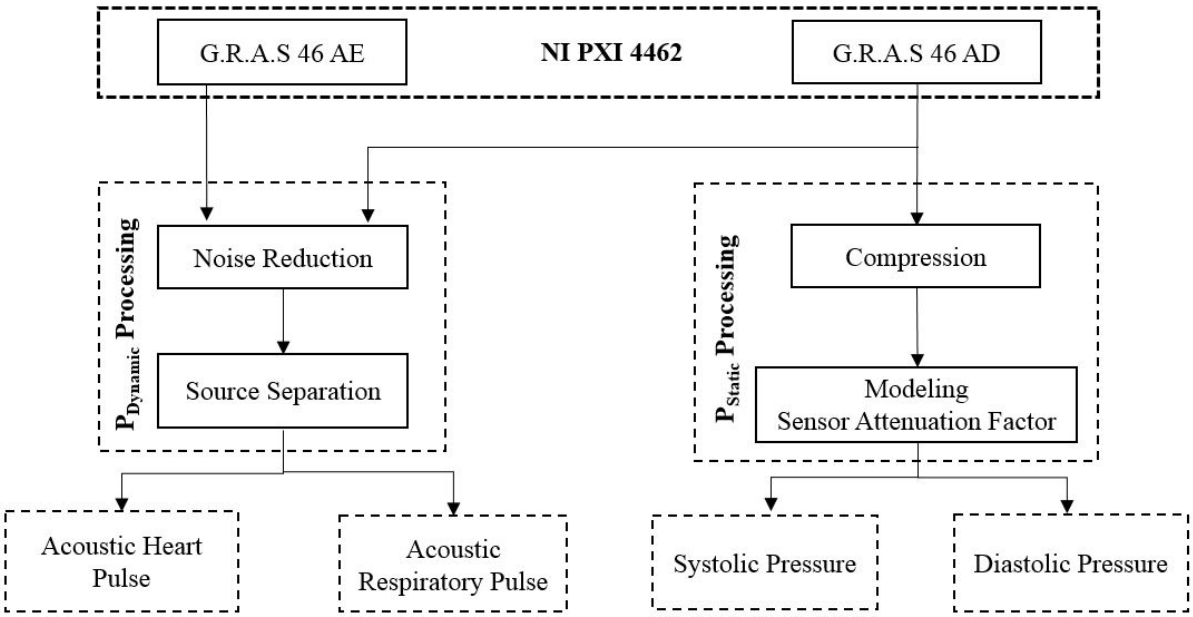

Figure 4.1: Signal Processing Framework to Extract Vital Bio-signals from the Blood Flow Dynamics.

4.2 Acoustic Heart and Respiratory Pulse Computation Framework

Analysis and processing of $P_{dynamic}$ is viewed as a problem that requires a combination of active noise cancellation and source separation for SNR improvement and bio-signal extraction. $P_{dynamic}$ is the result of acoustical sound pressure created by the oscillation of the blood column at the boundary of the barrier. Effectively, it is the sound of the blood flow or the acoustic field of the blood flow. Since the measurement was made in a noisy clinical setting, the blood flow sound was interfered by other acoustical sources present in the setting. Thus, in order to extract the bio-signals with fidelity from this measurement, the acquired $P_{dynamic}$ needed to be enhanced using a noise cancellation technique. Further, a comparative performance evaluation of spectral subtraction and various Least Mean Squares (LMS) based adaptive noise cancellation techniques was accomplished based on Noise Factor (NF) and Signal to Noise Ratio (SNR). In order to extract multiple bio-signals from the noise enhanced signal, a source separation technique based on Multiresolution Analysis (MRA) was also developed. The block diagram of the developed framework for processing the blood flow acoustics is shown in Figure 4.2. In Figure 4.2, measurements from the G.R.A.S 46 AD and 46 AE microphones are processed using noise cancellation and source separation blocks to obtain the vital bio-signals.

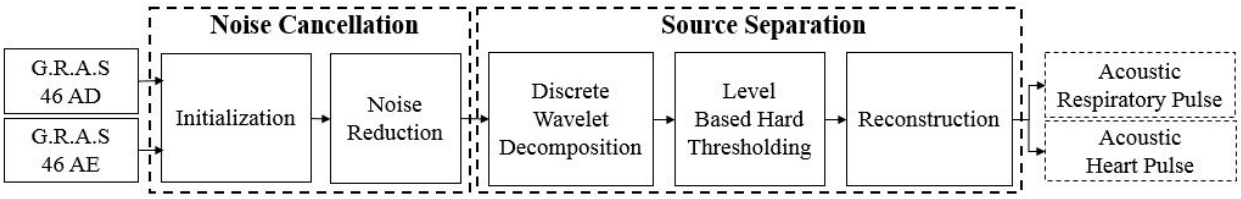

Figure 4.2: Overview of Blood Flow Sound Processing.

4.2.1 Noise Cancellation

In the noise cancellation block, the microphone measurements are subject to initialization where the data is decimated and segmented into frames. Then, the segmented data from both

channels is processed using noise reductions algorithms that include spectral subtraction and LMS based adaptive noise cancellation algorithms as described in the following subsections.

4.2.1.1 Spectral Subtraction

Spectral subtraction is a widely employed technique in applications that require cancellation of interference from acoustic noise. Many studies used a single channel spectral subtraction technique that assumed stationarity of the noise in order to improve the SNR of the sound pressure measurement [66, 67, 68]. However, it has been shown by studies [69, 70] that a multichannel spectral subtraction is not only computationally simple but also very efficient in improving the SNR of sound pressure measurements, particularly when a part of the reference acoustic noise is assumed to be superimposed into the sound pressure measurement by means of an unknown system as shown in Figure 4.3. The fluid filled catheter and the waveguide from the data acquisition system, as shown in Figure 3.3, were identified as the major components of the system with unknown impulse responses through which the noise, n(n), that is correlated to the reference acoustic noise, $n_0(n)$, gets superimposed onto the desired signal, x(n). In this study, a spectral magnitude subtraction technique was implemented to remove the noise superimposed onto the data channel. Figure 4.3 shows the block diagram of the implemented spectral subtraction algorithm.

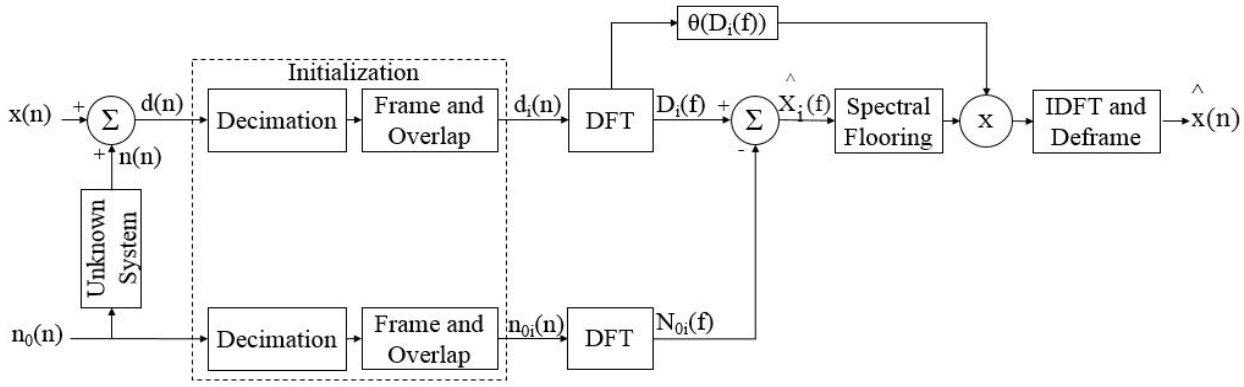

Figure 4.3: Block Diagram Representation of the Implemented Spectral Subtraction Algorithm.

In Figure 4.3, the implemented spectral subtraction algorithm includes a data channel that measures the acoustic field of the blood flow dynamics, d(n), where n is the sample index, and a noise channel that measures reference acoustic noise from the clinical setting, $n_0(n)$. The noisy measurement, d(n), acquired in the data channel is a result of superimposition of the desired signal, x(n) and a manifestation of the reference acoustic noise, n(n). Equation (4) provides time domain model for the noisy measurement.

$$d(n) = x(n) + n(n) \tag{4}$$

Here, d(n) and $n_0(n)$ were passed through an initialization block that decimated the signals from 10 kHz to 1 kHz and then segmented to 2 second long frames with 80% overlap. Each data frame, $d_i(n)$, where i is the frame index, and noise frame, $n_{0i}(n)$, was windowed using a rectangular window and transformed into the frequency domain using the Discrete Fourier Transform (DFT). Then, each incoming frequency transformed data frame, $D_i(f)$, and noise frame, $N_{0_i}(f)$, were subjected to magnitude spectral subtraction to provide an estimate of the desired signal $|\hat{X}_i(f)|$ as shown in equation (5).

$$\left|\hat{X}_i(f)\right| = |D_i(f)| - \left|N_{0_i}(f)\right| \tag{5}$$

Equation (5) resulted in processing distortions by producing negative values in the estimated magnitude spectrum owing to the variations of the noise channel spectrum. Hence, the estimated magnitude spectrum, $|\hat{X}_i(f)|$, is processed by the spectral flooring function to prevent negative values in the estimated magnitude. Equation (6) presents the function that was used to perform spectral flooring [66, 71].

$$|\hat{X}_i(f)| = \begin{cases} 0.01|D_i(f)| & \text{if } |\hat{X}_i(f)| < 0 \\ |\hat{X}_i(f)| & \text{otherwise} \end{cases} \tag{6}$$

The spectral floored magnitude spectrum estimate,$|\hat{X}_i(f)|$, is combined with the phase of the noisy signal spectrum, $\theta(D_i(f))$, and then transformed into the time domain via the Inverse DFT (IDFT). Finally, concatenating the outputs from the IDFT yielded an estimate of the desired signal $\hat{x}(n)$.

4.2.1.2 Adaptive Noise Cancellation

Adaptive noise cancellation is another widely used multichannel noise cancellation technique to remove acoustic noise interference. In particular, the current research evaluates the performance of the various adaptive noise cancellation algorithms in such a configuration where a part of the reference acoustic noise is assumed to be superimposed onto the data channel as shown in Figure 4.4. In order to determine the best noise cancellation technique, the performance of the LMS, sign LMS, normalized LMS and fast block LMS algorithms were compared with spectral subtraction.

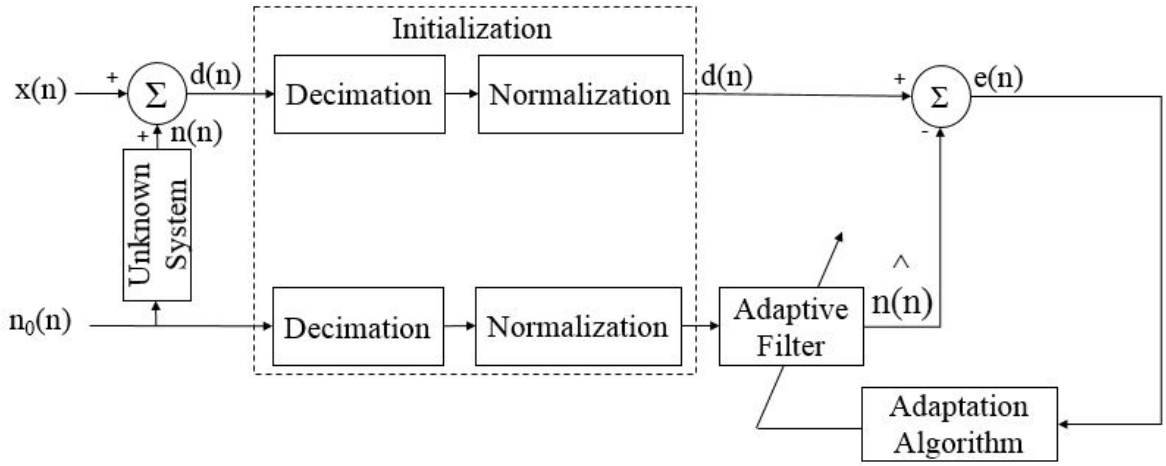

Figure 4.4: Block Diagram Representation of the Implemented Adaptive Noise Cancellation Algorithm.

The configuration considered in Figure 4.4 is similar to the case that was considered for the spectral subtraction based noise cancellation; where the noisy measurement, d(n), acquired in the data channel is a result of superimposition of the desired signal, x(n), and a manifestation of

the reference acoustic noise, n(n), as shown in equation (4). It is the assumption that the desired signal, x(n), is statistically independent of n(n) and $n_0(n)$; n(n) and $n_0(n)$ are correlated in some sense. In this algorithm, both d(n) and $n_0(n)$ were passed through an initialization block that decimated the signals from 10 kHz to 1 kHz and then normalized. The normalized noise, $n_0(n)$, is filtered to produce $\hat{n}(n)$, an estimate of n(n) using minimum mean square estimation. Equations (7), (8), and (9) represent filtering, error computation and weight update operations of the LMS based adaptive noise cancellation algorithm, respectively.

$$\hat{n}(n) = w^T(n) * n_0(n) \quad (7)$$
$$e(n) = d(n) - \hat{n}(n) \quad (8)$$
$$w(n+1) = w(n) + \mu\, x(n)e(n) \quad (9)$$

In equation (7), $w^T(n)$ represents the computed coefficients of the adaptive filter based on the order (M), μ provides the step size for the weight update operation, e is the computed error which is considered to be the noise free estimate $\hat{x}(n)$ and n is the sample index. In the current study, M was set to 300 and μ was set to 0.01 for LMS. Sign LMS and normalized LMS were implemented using (10) and (11), respectively.

$$w(n+1) = w(n) + \mu\, sign(x(n))e(n) \quad (10)$$
$$w(n+1) = w(n) + \frac{\mu^2}{\Delta + \sigma^2_{n_0(n)}}\, x(n)e(n) \quad (11)$$

In equation (10), *sign* represents a standard signum function. In equation (11), Δ is a constant and σ is the standard deviation of $n_0(n)$ which depends on the order of the filter. For sign LMS, M was set to 300 and μ was set to 0.01. For normalized LMS, M was set to 300, μ was set to 0.3 and Δ to 0.1. The block LMS was implemented using a Fast Fourier Transform (FFT) based algorithm as described in [72]. The μ was set to 0.5, the block size and M were set to 300, the forgetting factor (γ) and initial average power estimate (P) were set to 0.1.

4.2.1.3 Performance Comparison of Noise Cancellation Algorithms

In order to assess the performance of the implemented noise cancellation techniques, evaluation metrics based on the NF and the SNR estimated averages were computed after application of each noise cancellation technique. The average of NF is estimated between the corresponding variances (σ^2) of d(n) and $\hat{x}(n)$. Prior to computing the averages of NF and SNR, an estimate of the noise $\hat{n}(n)$ is computed by subtracting $\hat{x}(n)$ resulting from the noisy measurement, d(n). Then, the SNR is estimated between the corresponding variances (σ^2) of noise free estimate $\hat{x}(n)$ and $\hat{n}(n)$. It should be noted that, d(n), $\hat{x}(n)$ and $\hat{n}(n)$ were segmented into 2 second long frames with 80% overlap before estimating the averages of NF and SNR. In the equations (12) and (13) i, v, and l represent frame index, number of frames and frame length respectively. NF is the ratio of powers of the noisy signal, $d_i(n)$, to the noise free signal, $\hat{x}_i(n)$. On the other hand, SNR is the ratio of powers of noise free signal, $\hat{x}_i(n)$, to the estimated noise, $\hat{n}_i(n)$.

$$\text{NF} = \frac{1}{v}\sum_{i=1}^{v} 10\log\left[\frac{\sigma^2_{|d_i(n)|}}{\sigma^2_{|\hat{x}_i(n)|}}\right] \tag{12}$$

$$\text{SNR} = \frac{1}{v}\sum_{i=1}^{v} 10\log\left[\frac{\sigma^2_{|\hat{x}_i(n)|}}{\sigma^2_{|\hat{n}_i(n)|}}\right] \tag{13}$$

Table 4.1 shows the estimated averages of NFs and SNRs corresponding to the spectral subtraction, LMS, sign LMS, normalized LMS and fast block LMS algorithms respectively. Lower value of the estimated NF and higher value of estimated SNR are indicative of greater proportion of noise being removed. Hence in comparison, the algorithm that provides a lowest value of NF and a highest value of SNR is considered to be performing better.

Table 4.1: Estimated Average NFs and SNRs.

Noise Cancellation	NF(dB)	SNR(dB)
Spectral Subtraction	20.54	-8.16
LMS	25.43	-9.75
Sign LMS	22.46	-8.48
Normalized LMS	25.12	-9.76

Table 4.1 (Contd.).

Fast Block LMS	25.38	-9.20

After application of spectral subtraction, P_{total} shows an average estimated SNR of -8.16 dB. Figure 4.5a shows the noisy measurement that was recorded at a critical care setting using the G.R.A.S 46 AD microphone. The noisy data is corrupted mainly due to acoustical artifacts generated from background speech, critical and emergency care instruments such as mechanical ventilator and the patient monitors. Specifically, it was observed that a very low frequency periodic noise due to a combination of hissing and thumping sounds was generated by the mechanical ventilator. This periodic artifact left a significant impact on the SNR of the measurement which can be seen around 10 and 50 seconds in Figure 4.5a. Spectral subtraction also provided considerable attenuation to the artifacts (see Figure 4.5b). On the other hand, the average estimated SNR of P_{total} after adaptive noise cancellation based on LMS and sign LMS were found to be -9.75 and -8.48 dBs, respectively. Figures 4.5c and 4.5d show the resultant outputs of LMS and sign LMS. With respect to normalized LMS and fast block LMS, the post noise cancellation average estimated SNR were found to be -9.76 and -9.20 dBs, respectively. Specifically, normalized LMS and fast block LMS have not provided considerable artifact attenuation in comparison to other noise cancellation techniques. See Figures 4.5e and 4.5f.

Though sign LMS quantitatively provides almost similar performance to that of spectral subtraction, spectral subtraction outperformed the sign LMS in attenuating the artifacts and providing better estimates of NF and SNR especially in the periods of d(n) where the artifact is not present. Thus, it was concluded that the spectral subtraction provides efficient performance in estimating x(n) from d(n) compared to the LMS, sign LMS, normalized LMS and fast block LMS algorithms.

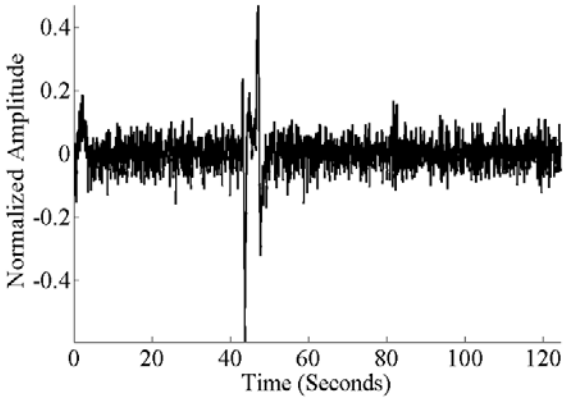

Figure 4.5a: Noisy Measurement.

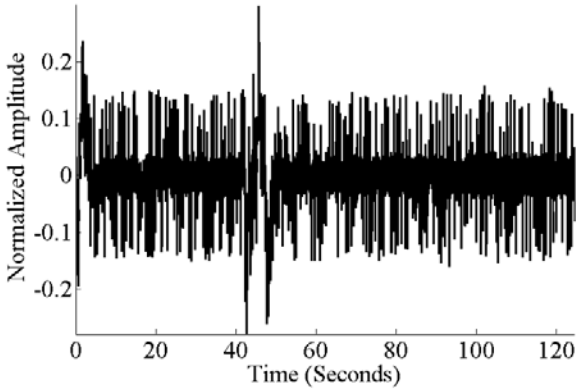

Figure 4.5b: SNR Enhanced Signal Using Spectral Subtraction.

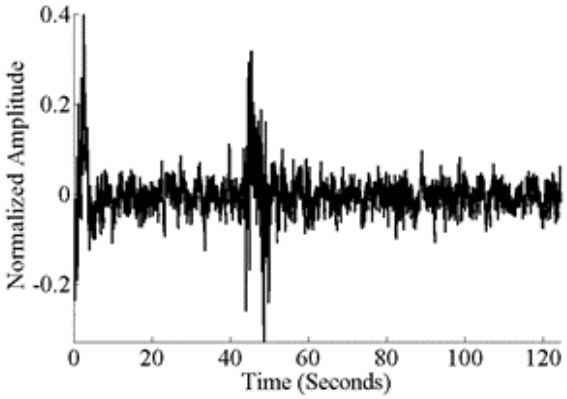

Figure 4.5c: SNR Enhanced Signal Using LMS Based ANC.

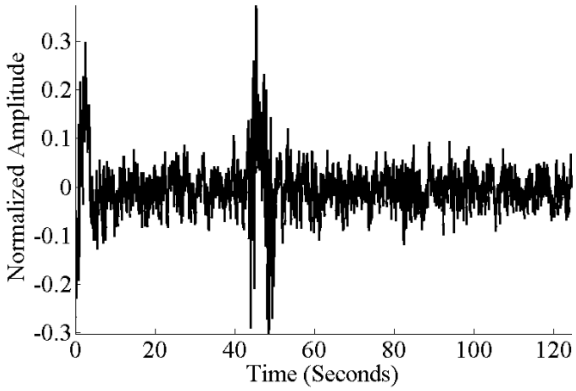

Figure 4.5d: SNR Enhanced Signal Using Sign LMS Based ANC.

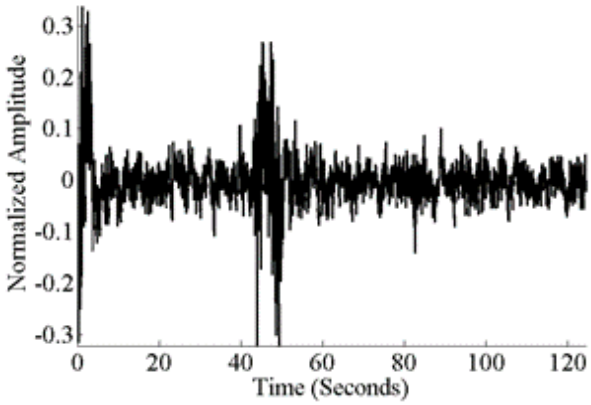

Figure 4.5e: SNR Enhanced Signal Using Normalized LMS Based ANC.

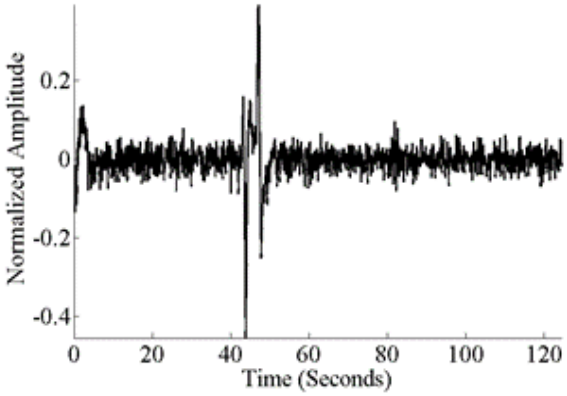

Figure 4.5f: SNR Enhanced Signal Using Block LMS Based ANC.

4.2.2 Source Separation

The noise reduced signal is then processed using the source separation block. This single channel observation is decomposed into various levels using discrete wavelet transform where only vital bio-signals of interest are then hard thresholded and reconstructed back. The details of these blocks of source separation are described in the following subsection.

4.2.2.1 Wavelet Based Source Separation

Preliminary results of Hashiodani *et al.* [73] indicated that analyzing the sounds acquired from an arterial body site can potentially include information with respect to bio-signals like heart sounds, sounds of blood stream, and respiratory sounds. As a result, it was assumed that the analysis of enhanced $P_{dynamic}$, i.e., sound of blood flow, would provide information with respect to bio-signals like heart and respiratory sounds. In this context, studies [74, 75] that used time-frequency transformation techniques to localize heart sounds from respiratory sounds have shown promising results especially for single channel source separation. Therefore, in this study a wavelet based MRA has been implemented in order to unmask the underlying bio-signals. In MRA, the given signal $\hat{x}(n)$, i.e., SNR enhanced $P_{dynamic}$ is decomposed into various levels of approximation (A) and detail (D) coefficients according to equation (14).

$$\begin{aligned} A_m(n) &= < \hat{x}(n), \varphi_{mk}(n) > \\ D_m(n) &= < \hat{x}(n), \psi_{mk}(n) > \end{aligned} \tag{14}$$

where <·> operator represents inner product, m represents the decomposition level, k represents the translation, ψ represents the mother wavelet with R vanishing moments and φ corresponds to its scaling function. In order to obtain the approximations and details of the subsequent levels, the wavelet (ψ) and scaling (φ) functions are represented as recursive functions given in equation (15) [76].

$$\psi(n) = \sum_{p=-\infty}^{\infty} h(p)\ \varphi(2n - p)$$
$$\varphi(n) = \sum_{p=-\infty}^{\infty} g(p)\ \varphi(2n - p) \qquad (15)$$

In equation (15), h(p) and g(p) are impulse responses of low pass and high pass quadrature mirror filters, respectively. The approximation and detail coefficients at each level are a result of the convolution between the signal $\hat{x}(n)$ with the impulse responses of h(p) and g(p). The approximation coefficients obtained at each level are down sampled by a factor of two and decomposed further into finer approximations and details. This process was continued until all the levels of the MRA were reached. After all the approximation and detail coefficients were obtained from the MRA, the coefficients corresponding to all the scales were set to zero except for the coefficients of the interest in a particular level. This hard thresholding process has been adopted in this current study to unmask bio-signals in the wavelet domain. Finally, after application of the thresholding, the new coefficients were reconstructed back into the time domain. Both the acoustic heart and respiratory pulses exhibit a different behavior in the wavelet domain in the sense that the acoustic heart pulses are highly dynamic and non-stationary; on the other hand, acoustic respiratory pulse is relatively slow varying [75]. Therefore, the chosen mother wavelet (ψ) should provide a reasonably good low and high frequency resolution to the underlying bio-signals of $\hat{x}(n)$ through compact support. Additionally, the lower cutoff frequency of the pressure field microphone was set to 3.15 Hz. Therefore, any underlying bio-signals of interest that contained frequency components below 3.15 Hz would have been attenuated and appeared as discontinuities in the measured pressure data. As a result, the chosen ψ need to be able to detect the presence of hidden discontinuities. Finally, the ψ should be orthogonal to avoid phase

distortions from the transformation. All the requirements of the current study were satisfied by the Coiflet wavelet with four vanishing moments.

4.2.2.2 Results of Source Separation

The estimate $\hat{x}(n)$ from spectral subtraction was subjected to MRA using fourth order Coiflet wavelet. The level of decomposition at which the detail coefficients were retained was bio-signal dependent and thus for acoustic heart pulses the coefficients of interest were identified at level four and for acoustic respiratory pulses the coefficients of interest were identified at level ten. Following the ten level MRA decomposition, coefficients of interest in a particular level were retained and a hard threshold was applied to coefficients corresponding to other scales. The acoustic heart and respiratory pulses masked in $\hat{x}(n)$ were extracted by performing a hard threshold on MRA coefficients, simultaneously retaining details coefficients of level four (D4), level ten (D10) and reconstructing them individually back into the time domain. Figures 4.6a and 4.6b show the extracted acoustic heart and respiratory pulses obtained after reconstruction.

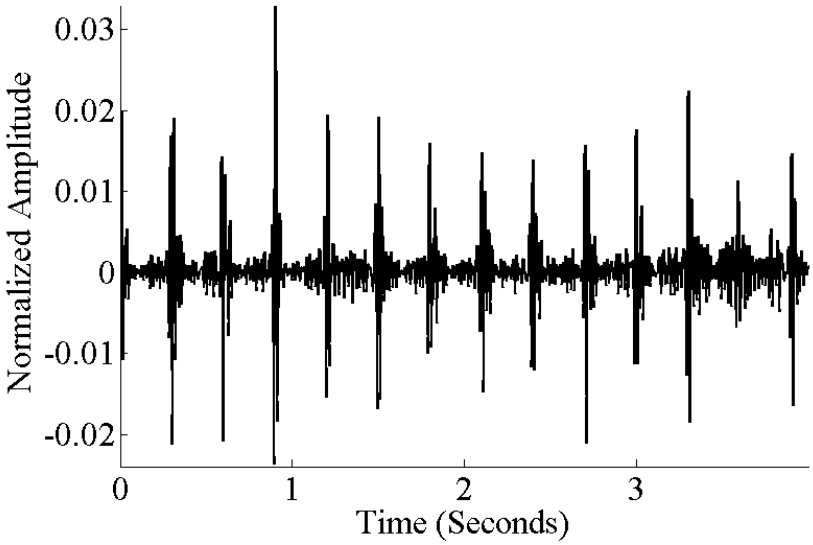

Figure 4.6a: Extracted Acoustic Heart Pulses.

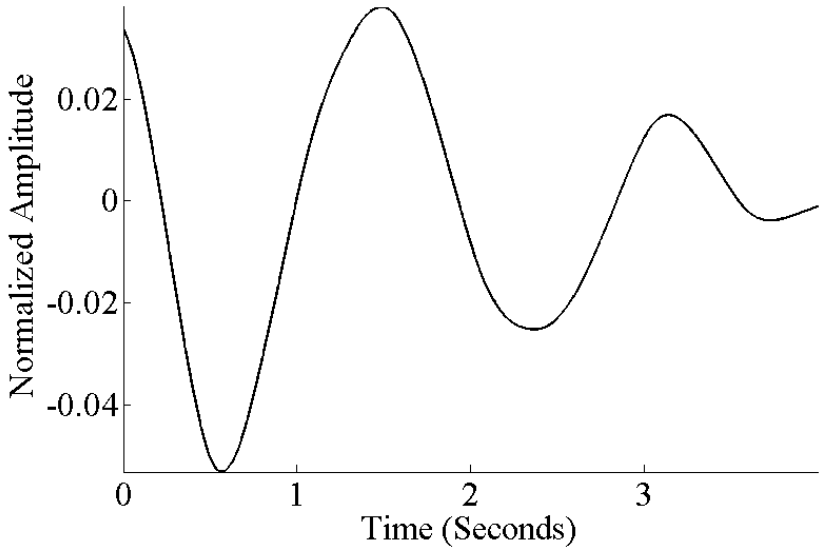

Figure 4.6b: Extracted Acoustic Respiratory Pulses.

The acoustic heart pulses were benchmarked by computing average heart rate in beats per minute (bpm) and comparing it to the average of heart rate that was recorded prior and post-acquisition of the noisy measurement. Since the acoustic respiratory pulse is a slowly varying waveform, further analysis was done on a relatively large time period. A first order sample difference was computed in order to identify the presence of any discontinuities that may have been present due to the bandlimited frequency response of the pressure field microphone. The corresponding results are shown in Figure 4.7.

From Figure 4.7, it can be observed that the slow moving respiratory signal was attenuated and discontinuities were introduced due to this attenuation. The number of discontinuities present were in direct correlation to the average respiratory rate in breaths per minute (rpm) acquired prior and post the d(n) acquisition for the purpose of benchmarking. The discontinuities can also be identified using MRA. The extracted acoustic respiratory pulse was decomposed into first level approximation and detail coefficients using fourth order Coiflet wavelet to obtain similar results.

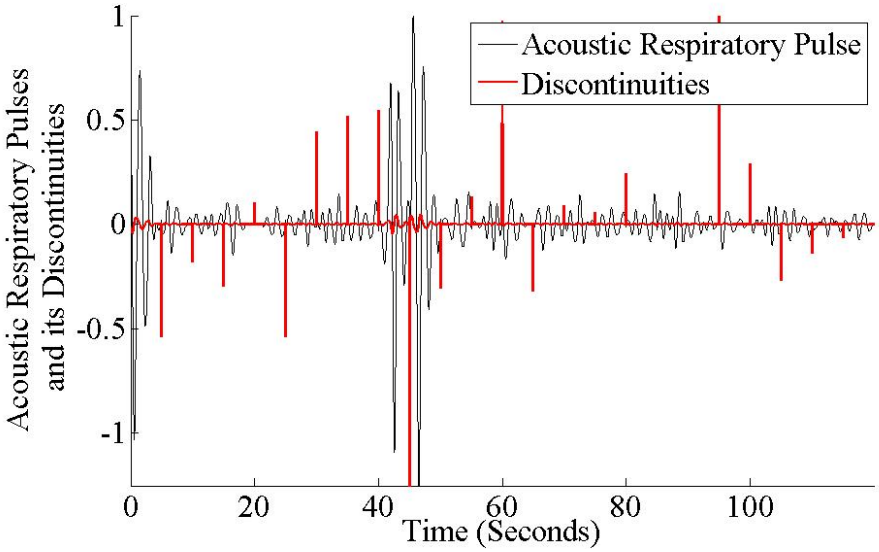

Figure 4.7: Acoustic Respiratory Pulse and the Corresponding Discontinuities.

4.2.2.3 Validation

Table 4.2 presents the error analysis results of computed heart and respiratory rates benchmarked with modalities obtained using conventional devices for all the venous and arterial blood flow dynamics given in Table 3.1.

Table 4.2: Error Analysis Results of Heart Rate and Respiratory Rate Benchmarking.

Index	Heart Rate (bpm)			Respiratory Rate (rpm)		
	Recorded Value	Computed Value	Error (± %)	Recorded Value	Computed Value	Error (± %)
1a	95	99	3.78	10	10.5	5
5a	110.5	102		10	10	
6a	128	120		10	11	
1b	218	210	0.59	10	11.5	15
5b	216.5	217.5		10	11.5	
6b	222	225		10	11.5	
2b	108.5	105	1.87	10	11	13
3a	116	112.5		10	11.5	
4b	96.5	97.5		10	11.5	
2a	179	180	2.38	10	10	5
3b	200	195		10	11	
4a	204.5	194.6		10	10.5	

The error percentage computed by benchmarking with conventionally measured modalities validate the extracted acoustic heart and respiratory pulses. From Table 4.2, it was observed that

the novel catheter multiscope measures the heart rate with an estimated error less than 4%, i.e., with higher precision when compared to the current heart rate monitors [77]. With respect to the respiratory rate, the proposed catheter multiscope recorded the largest estimation error of 15% (1.5 rpm), which is within the acceptable tolerance and can be regarded as a comparable measurement to an optimized respiratory rate monitor [78].

4.3 Continuous Blood Pressure Computation Framework

Continuous blood pressure was extracted from P_{total} following a novel signal processing framework shown in Figure 4.8. Even though static pressure was equalized, it was observed that measured P_{total} consisted of traces of P_{static} due to the insufficient discharge time constant of the pressure field microphone. Making use of this limitation, normalized blood pressure was extracted, i.e., P_{static} was extracted by computing the local mean for every 25 ms from the measured P_{total}. This local mean computation effectively compressed the number of data samples of P_{total} from 10000 samples to 40 samples for each second. The segment length for mean computation was deliberately chosen to be 25 ms since all the harmonics of blood pressure signal are present between 0 to 20 Hz. Extraction of P_{static} from P_{total} resulted in normalized blood pressure. The computed normalized blood pressure was further validated by establishing comparison between the human and animal blood pressure data. This comparison was accomplished by estimating the magnitude squared coherence between the normalized blood pressure data derived from recording index 1a and the Physionet arterial blood pressure derived from a mutli-parameter waveform database using Welch's overlapped segment averaging.

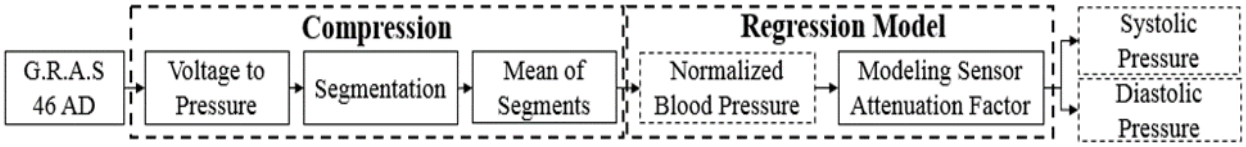

Figure 4.8: Overview of Continuous Blood Pressure Computation Framework.

4.3.1 Blood Pressure Estimation and Validation

From the extracted normalized blood pressure, it is not possible to directly estimate the systolic and diastolic pressure. To estimate pressures, the pressure field microphone attenuation factors k_1, k_2 corresponding to systolic and diastolic pressures were first estimated using the regression model shown in equation (16), where sys is the systolic pressure, dia is the diastolic pressure, M is the mean arterial pressure obtained using the conventional devices, P is the local maxima and V is the local minima of the normalized blood pressure obtained after compression of P_{total}. k_1 and k_2 are the sensor attenuation factors corresponding to the systolic and the diastolic pressures.

$$\begin{aligned} sys &= k_1 \,.\, (P + M) \\ dia &= k_2 \,.\, (V + M) \end{aligned} \tag{16}$$

The regression model first estimates the systolic and diastolic attenuation factors using the blood pressure data obtained from conventional instruments, i.e., M, sys and dia. The systolic and diastolic pressures were then estimated using the computed regression model. The sensor attenuation factors k_1 and k_2 were computed using the normalized blood pressure data for recording indices 1a to 6b. The factors k_1 and k_2 were found to be 1.1078 ± 0.0658 and 0.8854 ± 0.0449, respectively. Later, the mean values of the obtained k_1 and k_2 are used to compute average systolic and diastolic pressures using equation (16) for all the recording indices from 1a to 6b as shown in Table 4.3.

Table 4.3: Error Analysis Results of Systolic and Diastolic Pressures Benchmarking.

Recording Index	Systolic Pressure (mmHg)			Diastolic Pressure (mmHg)		
	Recorded Value	Computed Value	Error (± %)	Recorded Value	Computed Value	Error (± %)
1a	84.5	82.5	3	63	65.96	1.5
5a	45	41		31.5	32.6	
6a	39	39.9		34	31.9	
1b	189.5	196.6	5	152.5	157.2	1.9
5b	181	187.8		152.5	150.1	
6b	141	152.9		133	122.2	
2b	52.5	49.9	5.6	39	39.8	4.2
3a	44.5	42.1		30.5	33.6	
4b	51	47.6		37.5	38.1	
2a	124	135.7	4.1	110	108.5	2.4
3b	171.5	175.6		143	140.3	
4a	186.5	190.5		158	152.3	

From Table 4.3, it can be observed that the novel catheter multiscope is able to predict systolic pressures with an estimated average error rate less than 6% and diastolic pressures with an estimated average error rate less than 5% in comparison to the current gold standard. It should be noted that, at this point results obtained for continuous blood pressure are considered to be preliminary since the systolic and diastolic pressures have been approximated from a sensor attenuation factor model. Additional benchmarking was accomplished with a human blood pressure data to confirm the validity of described blood pressure estimation approach. Details are provided in Appendix A.

CHAPTER 5: APPLICATION CASE STUDIES

5.1 Sinus Rhythm Pattern Recognition[3].

5.1.1 Background

The centers for disease control and prevention estimates that more than 600,000 people die of heart diseases every year in United States [79]. In addition to this overwhelming number of heart disease cases, critical care units in the United States have reported a 90% false arrhythmia alarm rate. Blood pressure, heart and respiratory rates are among other vital bio-signals that are acquired and monitored in critical care units [80]. No other comparable studies in the literature have described a diagnostic system that is capable of providing multiple vital bio-signals and detecting an arrhythmia. Hence, our motivation is to develop a multiple bio-signal feature extraction and pattern recognition framework for biomedical acoustic signals. In order to demonstrate the feasibility of the developed framework, preliminary results are presented by processing the acoustic heart pulses of the catheter multiscope

The blood flow sounds collected from various body sites in the current case study under the conditions of normal and abnormal sinus rhythms are analyzed using an extended version of the previously validated signal processing framework. See Figure 4.2. The extended framework, initially extracts the acoustic heart and respiratory pulses from the measured blood flow sounds

[3]A preliminary version of the content presented in Chapter 5, section 5 has been published in proceedings of 2017 International Conference of Software and Smart Convergence [125] and NIH-IEEE 2017 Special Topics conference on Healthcare Innovations and Point of Care Technologies: Technology in Translation [124].

using a noise cancellation and wavelet source separation technique based preprocessing. Then, the extracted acoustic heart pulses are post processed to recognize the patterns of the sinus rhythm based on a novel feature extraction technique and cluster analysis. The developed framework was qualitatively and quantitatively validated by providing visual results of the clustering and by computing the clustering accuracy, sensitivity and specificity. The cross validation results show that the developed framework consistently recognizes the patterns of the sinus rhythms with an accuracy rate of 94.37%.

5.1.2 Pattern Recognition Framework

Analysis and processing of the acquired dynamic pressure, i.e., blood flow sounds, was viewed as a problem that requires a combination of preprocessing, feature extraction and clustering. Since the measurement was made in a noisy clinical setting, measurement of this blood flow sound was interfered by other acoustical sources present in the setting. Thus, in order to extract the bio-signals with fidelity from this measurement, noise had to be reduced using a spectral subtraction based noise cancellation technique. Next, the noise reduced signal was preprocessed with the wavelet source separation in order to extract acoustic heart and respiratory pulses. Later the extracted acoustic heart pulses were segmented; features were extracted and the pattern was then recognized from the extracted features. The developed feature extraction and pattern recognition technique was able to independently cluster normal and abnormal sinus rhythm patterns of the acoustic heart pulses. Figure 5.1 shows the developed signal analysis and processing framework for biomedical acoustic signals. The acoustic heart pulses obtained by processing the signals of the catheter multiscope, as described in section 4.2 were processed further through feature extraction and pattern recognition. The features multiscale energy was extracted and then its pattern was recognized using K-Means clustering as explained in the following sections.

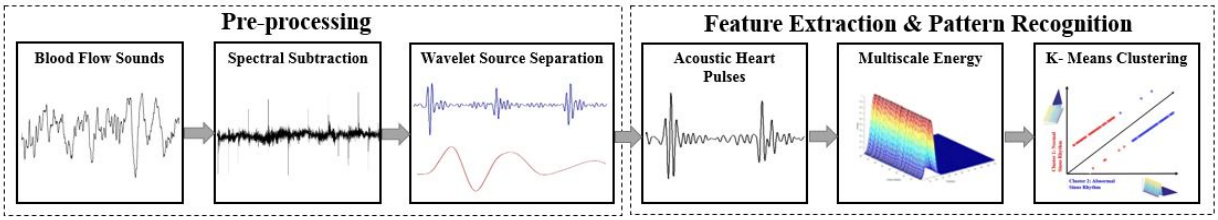

Figure 5.1: Biomedical Acoustical Signal Analysis and Processing Framework.

5.1.2.1 Feature Extraction and Cluster Analysis

5.1.2.1.1 Multiscale Energy

A Continuous Time Wavelet Transform (CTWT) based feature called multiscale energy was developed and computed for each segment of the acoustic heart pulse. The normalized CTWT of a continuous signal h(t) is given by equation (17).

$$W_{h;\psi}(\tau, s) = \frac{1}{\sqrt{s}} \int_{-\infty}^{\infty} h(t) * \psi^* \left(\frac{t - \tau}{s} \right) dt \tag{17}$$

Here W is the computed continuous wavelet transform, h(t) is a segment of the acoustic heart pulse, s is the scale coefficient associated to stretching or compression of the signal in time, τ is the translation parameter, ψ is the chosen mother wavelet [81]. The Multiscale Energy (ME) is computed using equation (18).

$$ME(s) = \sum_{\tau} \left| W_{h;\psi}(\tau, s) \right|^2 \tag{18}$$

The ME feature is computed at each scale of the CTWT of h(t) using Coiflet wavelet with four vanishing moments as chosen mother wavelet.

5.1.2.1.2 K-Means Clustering

K-means clustering algorithm was applied to ME features of the acoustic heart pulse segments for sinus rhythm pattern recognition. The following procedure adapted from [82] is implemented to cluster the ME features:

1. Input the computed ME feature vector set, v, of the extracted acoustic heart pulses to K-Means algorithm.

2. Randomly select the initial cluster centers from the feature set whose dimension is n_{b1} x n_{b2} x n_p x f_p. Here, n_{b1} represents the number of body sites, n_{b2} is the number measurements taken at each body site, n_p is the number of segments and f_p represents the number of features per segment or feature index, i.e., features computed based on the scale vector of the CTWT.
3. Assign the features that are closest to the cluster centroids according to the Euclidean distance function shown in equation (19) to the cluster number (j) depending on the maximum number of clusters, K, and n_{b1} x n_{b2} x n_p.

$$\sum_{j=1}^{K} \sum_{p=1}^{n_{b1} \times n_{b2} \times n_p} \left\| v_p^j - c_j \right\|^2 \tag{19}$$

4. Recompute the centroids based on the formed new clusters.
5. Iteratively repeat the steps 2, 3 and 4 until the Euclidean distance function reaches convergence.

5.1.3 Results and Discussion

After preprocessing the blood flow sounds, further analysis was done on the extracted acoustic heart pulses corresponding to normal and abnormal sinus rhythms. The extracted acoustic heart pulses were segmented into three second long segments and the ME features were computed for each segment of the acoustic heart pulses. It has to be noted that, the number of body sites is

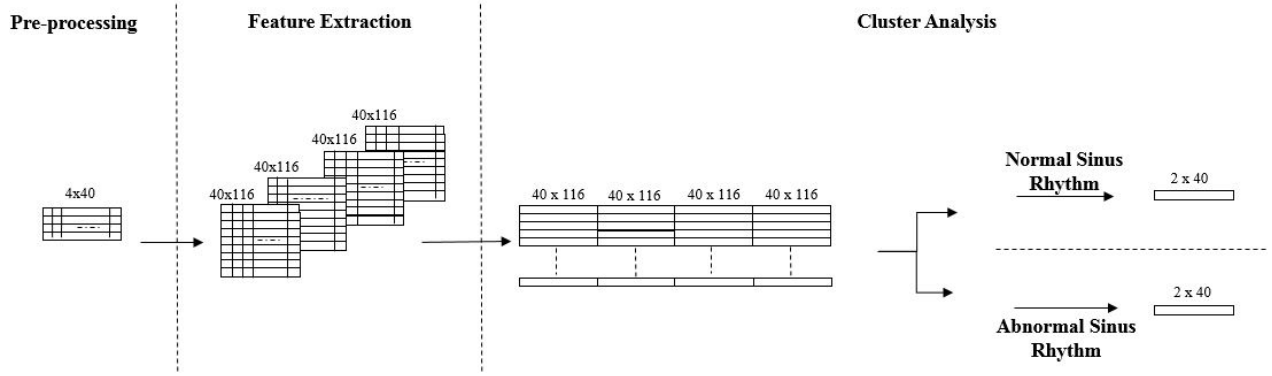

Figure 5.2: Feature Extraction and Pattern Recognition Dimensionality.

2; the number of measurements at each body site, n_{b2}, is 2; the number of segment instances, n_p, is 40 and the number of features per segment, f_p, is 116. Figure 5.2 is provided to show the dimensionality of the data when feature extraction and pattern recognition is performed.

Also, prior clustering, features corresponding to different body sites and sinus rhythm patterns were randomly grouped to obtain a final feature set with dimensions resulting in (2 x 2 x 40) x 116, where 2 x 2 x 40 is the segment index corresponding to acoustic heart pulses of both normal and abnormal sinus rhythms of carotid artery and jugular vein. Figures 5.3a and 5.3b show the ME features computed for acoustic heart sounds of normal and abnormal sinus rhythm segments of the carotid artery. In Figures 5.3a and 5.3b, each color represents the features (1x116) per segment. Figures 5.3a and 5.3b show the ME features computed for acoustic heart sounds of normal and abnormal sinus rhythm segments of the carotid artery. In Figures 5.3a and 5.3b, each color represents the features (1x116) per segment.

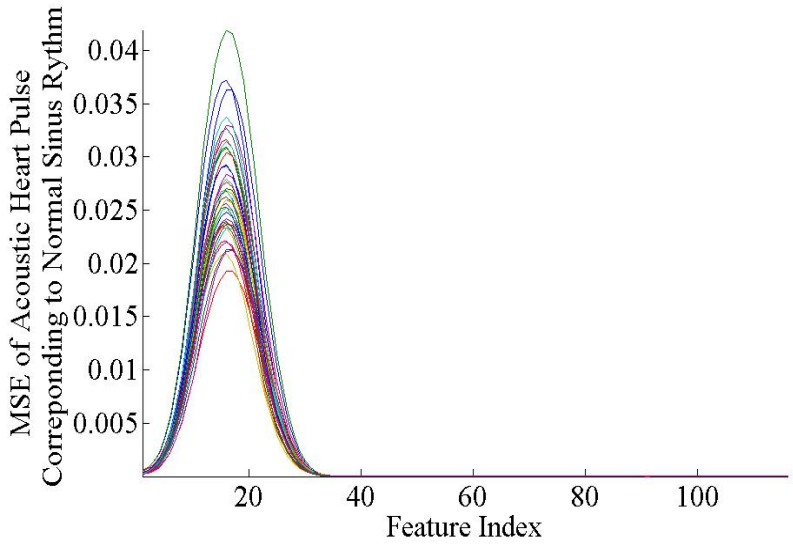

Figure 5.3a: ME of Acoustic Heart Pulse Corresponding to Normal Sinus Rhythm.

The computed ME features are scaled and separated into 2 clusters using Euclidean distance based K-means clustering algorithm. The cluster number (K) has been selected based on the average silhouette coefficient (C_p) computation given in [83]. The C_p for the data used in the

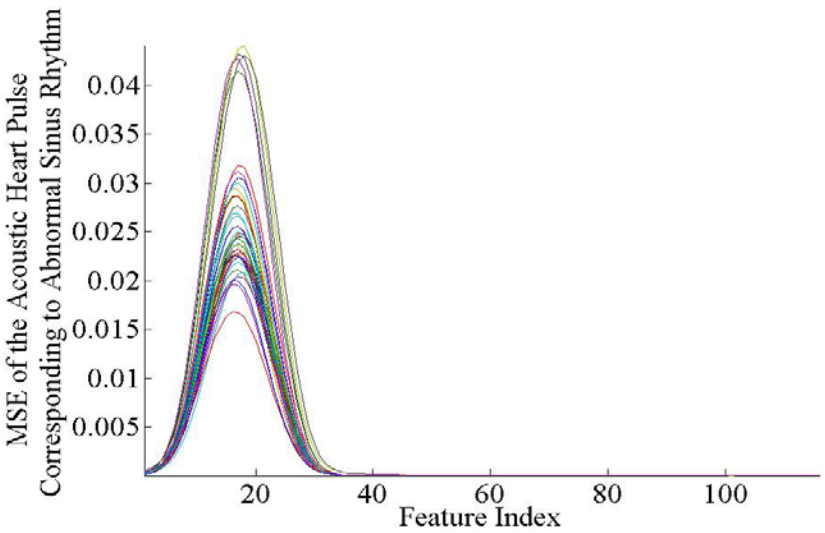

Figure 5.3b: ME of Acoustic Heart Pulse Corresponding to Abnormal Sinus Rhythm.

current case study was determined to be 2 which can be associated to clusters corresponding to normal and abnormal sinus rhythms. Figure 5.4 shows the qualitative results of K-means clustering.

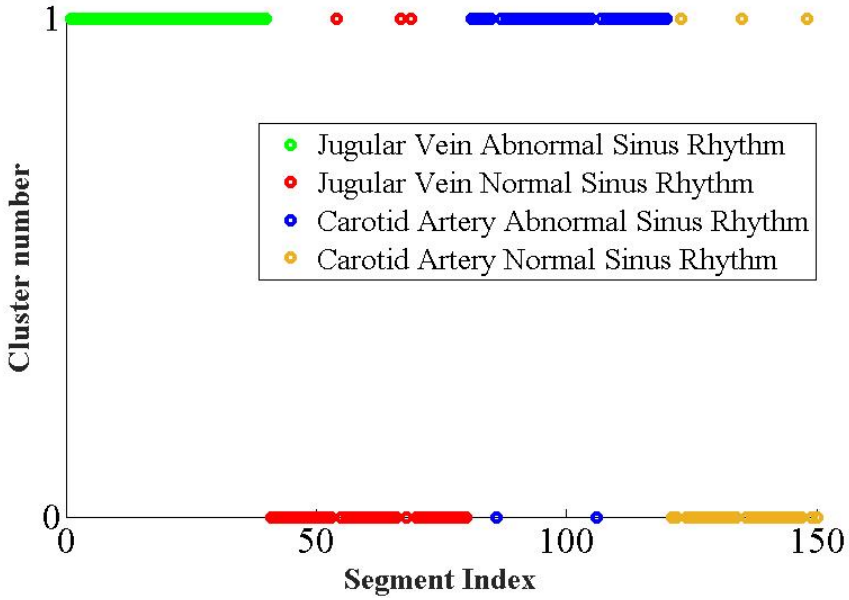

Figure 5.4: Qualitative Results of K–Means Clustering.

It can be observed from Figure 5.4 that K-means provides a satisfactory sinus rhythm pattern recognition by separating the ME features into two different clusters. To further validate

the developed ME features and the clustering framework, quantitative factors such as sensitivity, specificity and accuracy have been computed from a cross validation based confusion matrix. Cross validation was accomplished by mixing the final feature set and performing clustering on the mixed feature set. It has to be noted that the clustering was accomplished by randomizing the feature set mixture up to 10 times. Finally, average values of the quantitative factors of the confusion matrix were computed. Table 5.1 presents the averaged results of the confusion matrix of the cluster analysis.

Table 5.1: Confusion Matrix of the Cluster Analysis.

$n_p = 160$	**Sinus Rhythm: Normal**	**Sinus Rhythm: Abnormal**
Predicted: Normal Sinus Rhythm	TN = 73	FN = 2
Predicted: Abnormal Sinus Rhythm	FP = 7	TP = 78

The confusion matrix shown in Table 5.1 was computed for 160 segment instances. The segment instances corresponding to the normal sinus rhythm was defined as True Negative (TN), i.e., cluster number 0 and the abnormal sinus rhythm was defined as True Positive (TP), i.e., cluster number 1. Sensitivity and specificity were computed from Table 2 to show that the developed framework recognizes the patterns of the normal sinus rhythm with 91.25% precision and abnormal sinus rhythm with 97.5% precision. In addition, it was also noted that the overall ability of the developed framework in recognizing the patterns of the sinus rhythms was accurate to 94.37%.

5.2 Fetal Phonocardiography[4]

5.2.1 Background

The Centers for Disease Control and Prevention (CDC) estimates that more than one million fetal deaths occur in the United States per year [84]. Complications such as preterm delivery, hypoxia, intrauterine growth retardation and others, not only lead to fetal distress and neonatal death but also can cause risks to maternal health. There is a lesser knowledge about the incidence, etiology and prevention strategies for these complications; therefore it is critical to monitor the status of both fetal and maternal health throughout pregnancy. Consequently, Electronic Fetal Monitoring (EFM) was introduced in 1960s as a valuable tool for diagnosing Fetal Heart Rate (FHR) during the antepartum and intrapartum periods of pregnancy [85]. Today, EFM is used in 90% of the labor diagnosis procedures in the United States [86] and includes Electrocardiography (ECG), Phonocardiography (PCG), Pulse Oximetry, Magnetocardiogram (MCG) and Tocodynamometer. Organizations such as the International Federation of Gynecology and Obstetrics (FIGO), the American College of Obstetricians and Gynecologists (ACOG), the National Institute of Child Health and Human Development (NICHHD), the Royal College of Obstetricians and Gynecologists (RCOG), and the National Institute of Clinical Excellence (NICE) have standardized the use of EFM in conjunction with Maternal Uterine Contractions (MUC) known as Cardiotocography (CTG) to optimize the outcomes for the mother and the new born infant [87, 88].

Fetal Phonocardiography (FPCG) was discovered by the interventions of Marsac, Kergardec and Kennedy during the 17th century [89, 90]. Although FPCG was discovered many

[4]The contents in chapter 5, section 5.2 have been published in Journal of Biomedical Signal Processing and Control [117] and proceedings of 36th Annual International Conference of the IEEE Engineering in Medicine and Biology Society [126]

years ago, interest in this research has only occurred over the last few years. Currently, the application of FPCG is limited to FHR analysis and is seen as a noninvasive means for data acquisition; it is only used as a secondary diagnosis tool in the antepartum, and has never been utilized for complete clinical diagnosis. There are few reasons as to why FPCG is not clinically accepted for a complete diagnosis: First, the FPCG is very noisy, owing to the fact that the acquired signal is a mixture of fetal acoustic components, maternal acoustic components and many other noises. Second, the characteristics of the aforementioned components are highly dependent on the location of data acquisition, gestational age, fetal and maternal positions which result in signal non-stationarity; finally, the non-linear transmission medium dynamically morphs all the components to result in a narrow band signal. Today's standard of care in fetal monitoring suspects that the fetal heart rate is predictive of pregnancy complications [91]. As a consequence, EFM relies predominantly on FHR and does not incorporate the characteristics of the FPCG waveform in the assessment of fetal and maternal outcomes. The primary reason for the exclusion of this information from clinical practice is that the technology to measure the Fetal Heart Sounds (FHS) reliably is not yet available. Secondly, the existing signal processing techniques are unable to deliver a FHS signal from the acquired FPCG signal without considerable distortion.

5.2.2 State-of-the-Art in Fetal Monitoring

The technologies available to accomplish fetal monitoring are FPCG, Fetal Ultrasound, Fetal Electrocardiography (FECG) [20, 92], Fetal Magnetocardiography (FMCG) [93], Fetal Pulse Oximetry/Photoplethysmography (FPPG) [94] and Tocodynamometer/Intrauterine Pressure Catheter (IUPC) [95]. Among all these methods, ultrasound is regarded as the gold standard in fetal monitoring and is widely used during pregnancy and labor. When ultrasound is used to obtain biophysical profiles and images, typically during weeks 18 – 22, is known as echocardiography

[96]; when ultrasound is used in conjunction with tocodynamometer/IUPC, typically employed during labor and antepartum to acquire FHR and UC, is known as cardiotocography (CTG) [97]. Continuous fetal monitoring using ultrasound, particularly during labor, is highly challenging for two main reasons: the transducer of the ultrasound's data acquisition system needs frequent realignment, and the constant presence of a highly trained operator during data acquisition is required [98, 99]. Ultrasound technique is highly sensitive to movement, hence any maternal and or fetal movement is known to affect the ultrasound's beam reflection [100]. Also, long term and ambulatory fetal monitoring using ultrasound is inappropriate due to complexity of the instrumentation [100, 101]. Studies [101, 102, 103, 104] have shown that long-term and short-term variability of FHR obtained from ultrasound data are not as precise when compared to other techniques. Even if all the limitations of the ultrasound technique are rectified, ultrasound still exposes the fetus to radiation. The safety of the fetus from this radiation exposure remains a concern, due to the lack of evidence in the current literature [105, 106, 107, 108, 109, 110]. Besides these limitations, data obtained from FPCG contains more information on cardiac abnormalities and pathologies than ultrasound in relation to fetus and mother [111]; hence, the consideration of ultrasound as the gold standard is debatable. Most of the fetal cardiac abnormalities are believed to have some manifestation on the morphology of the FECG and the FMCG. However, they exhibit a poor Signal to Noise Ratio (SNR) due to unresolved maternal and bio-signal interferences [102, 103] and they have a complex instrumentation [102, 112, 113]. Traditionally, FECG is known for producing the highest quality measurement of FHR, but it has been shown within the literature that FHR from a FPCG signal is equally as reliable as FECG [114]. The use of FPPG is also restrained, as the light emitted from the signal is known to increase the fetal temperature, has a poor SNR due to the presence of ambient light and it has an optical

shunt problem [115]. Henceforth, the current standards of fetal monitoring are unreliable particularly during labor [116, 19]. On the other hand, though the FPCG has potential for fetal monitoring during first and second trimesters as well as labor, its usage as a secondary diagnosis tool is limited to antepartum as it suffers from low SNR due to maternal signal interference, maternal motion, nonlinear transmission medium and limitations in the existing data acquisition approaches and data acquisition systems. If the existing data acquisition approaches, data acquisition systems and signal processing techniques are improved, FPCG is capable of addressing all the limitations that the other methods present. Based on this observation, motivation for addressing the gaps of fetal monitoring through FPCG was found.

Acquisition, analysis, and processing of fetal heart sounds from maternal body is known as FPCG. The signal acquired at the transducer is a superimposition of various time varying acoustic and pressure components. Essentially it consists of fetal acoustic and pressure components: Fetal Heart Sounds (FHS), Fetal Movements (FM) that include Fetal Respiration (FR), fetal hiccups, and body movements; maternal acoustic and pressure components: Maternal Heart Sounds (MHS), Maternal Organ Sounds (MOS) that include Maternal Respiration (MR), Maternal Uterine Contractions (MUC), Maternal Digestive Sounds (MDS), and Maternal Motion (MM); additional signal components that include Power Line Interference (PLI), Reverberation Noise (RN), Sensor and Background Noise (SBN). These components provide invaluable diagnostic information about the fetal and the maternal health; however, its analysis and processing is rather challenging. In particular, the FHS signal has low SNR as it gets attenuated due to transmission path losses, and also gets superimposed with other fetal, maternal and additional components. Among all the components of FPCG, MHS overlap with FHS in both time and frequency domains. Further, fetal position, maternal obesity, placental position and location of

data acquisition play an important role in determining the SNR of the FHS signal and henceforth the SNR of the FPCG. For these reasons, denoising and recovering FHS from FPCG requires application of advanced signal processing algorithms.

In the literature, various signal processing techniques have been described to denoise the FPCG ranging from simple digital filters to advanced source separation techniques [117]. Though filtering and other heuristic methods are computationally efficient, these methods are not able to completely reduce the MHS interference in FPCG. Consequently, to solve the problem of MHS interference, adaptive filtering and blind source separation techniques have been implemented. However, these techniques require data that is captured from multiple channels in order to successfully denoise the MHS from FPCG and thus when it comes to single channel FPCG, these techniques do not perform well. Though specific blind source separation techniques have also been used to decompose FHS from a single channel FPCG, they fail to successfully retain time domain characteristics of the FHS, in particular FHR. In summary, the proposed techniques suffer to efficiently eliminate both the in-band and out-of-band noise present within a single channel FPCG.

In order to address these challenges, a single channel FPCG processing framework has been developed. This framework is capable of denoising the FPCG by accurately reconstructing FHS while efficiently removing the MHS and out-of-band interferences. The proposed framework first enhances the SNR of the noisy FPCG by removing the out-of-band noise using a single channel enhanced spectral subtraction technique. The performance of the implemented denoising algorithm is quantitatively assessed by computing Noise Factor (NF). Then, the SNR enhanced FPCG is decomposed into FHS and MHS in time-scale domain using a wavelet based source separation as shown for the catheter stethoscope in Figure 4.2. Finally, the recovered FHS and

MHS are quantitatively validated by computing FHR, Maternal Heart Rate (MHR) and comparing it to the standard values.

5.2.3 Fetal Phonocardiogram Processing Framework

Analysis and processing of a single channel FPCG signal was seen as a problem that requires a combination of noise cancellation and source separation for noise reduction and bio-signal interference resolution. The noise reduction technique was predominantly used to remove the out-of-band noise such as fetal movements, maternal organ sounds and additional components and in order to enhance the SNR of the noisy FPCG signal. A wavelet based source separation was implemented to decouple the MHS from FPCG, i.e., the in-band noise in order faithfully recover FHS. Figure 5.5 illustrates the framework that was used to process the single channel FPCG data. The simulated fetal phonocardiogram signals are processed using similar noise cancellation and source separation algorithms described earlier in section 4.2 and as shown in the block diagram in Figure 5.5. The framework was validated using the simulated FPCG dataset extracted from the PhysioNet database [118] [25]. Single channel FPCG signals corresponding to various SNR conditions were subjected to the developed framework to assess its reliability.

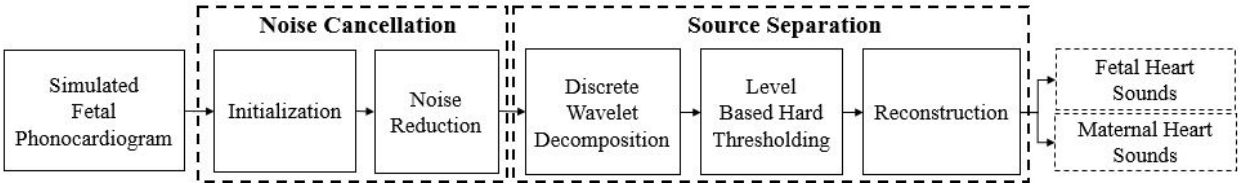

Figure 5.5: Fetal Phonocardiogram Processing Framework.

5.2.3.1 Noise Cancellation

In this case study, an enhanced spectral magnitude subtraction technique was implemented to remove the out-of-band noise superimposed onto the FPCG. Fetal movements, maternal organ sounds and additional components are the major contributors of the out-of-band noise. In the simulated FPCG dataset, the impulse responses of the out-of-band noise were identified to be either

Gaussian or impulse noise. In particular, MDS, MR, FM and SBN were the sources of the Gaussian noise; MM and RN were the sources of the impulse noise. The out-of-band noise is estimated and updated from the periods when the FHS and MHS are absent.

The implemented spectral subtraction algorithm includes a data channel that consists of noisy FPCG data, d(n), and a noise channel that estimates an ensemble average of the out-of-band from the data channel, n(n). The d(n) and the n(n) were passed through an initialization block that segmented to frames of length one second with 60% overlap between adjacent frames. Each data frame, $d_i(n)$, and noise frame, $n_i(n)$, where i is the frame index and n is the sample index, was windowed using a rectangular window and transformed into frequency domain using Discrete Fourier Transform (DFT). Then each incoming frequency transformed data frame, $D_i(f)$, and noise frame, $N_i(f)$, was subjected to magnitude spectral subtraction to provide an estimate of SNR enhanced FPCG signal, $\left|\hat{X}_i(f)\right|$, as shown in equation (5). Then the estimated signal is post processed using equation (6) to remove nulls in the spectral domains before performing inverse DFT.

5.2.3.2 Source Separation

In this case study, a wavelet based Multiresolution Analysis (MRA) has been implemented in order to extract the FHS and MHS from the FPCG. In MRA, the given signal, $\hat{x}(n)$, i.e., SNR enhanced FPCG is decomposed into various levels of approximation and detail coefficients. The approximation and detail coefficients obtained after the MRA were hard thresholded based on the bio-signal of interest and reconstructed back into time domain. The chosen mother wavelet should provide a reasonably good frequency resolution to FHS and MHS, through compact support. The mother wavelet needs to be able to detect the presence of hidden discontinuities. In addition, the wavelet should also be orthogonal to avoid phase distortions from the transformation. All the

requirements of the current case study were satisfied by the Coiflet wavelet with five vanishing moments. In addition, qualitative correlation between Coiflet-5 wavelet and the heart sounds, fetal and maternal, is very high.

5.2.4 Results and Discussion

In order to assess the performance of the developed noise cancellation algorithm, simulated FPCG data corresponding to various SNRs were quantitatively evaluated using NF after noise cancellation. Unavailability of the actual out-of-band noise n(n), FHS and MHS data was the main reason behind choosing NF as a performance evaluation metric. In this case study, average NF was estimated as ratio of variances of d(n) and $\hat{x}(n)$. It has to be noted that d(n) and $\hat{x}(n)$ were segmented into frames of length one second and with 60% overlap between adjacent frames, where i and v represent frame index, and number of frames before estimating the average NF as given in equation (12). Table 5.2 shows the noise removal consistency of the developed noise cancellation algorithm for various SNRs of the simulated FPCG data. Lower value of the NF indicates great proportion of noise being removed.

Table 5.2: Estimated Average Noise Factors for FPCG.

Standard Deviation of FPCG Noise (dB)	**Noise Factor (dB)**
73.12	-4.20
74.76	-3.28
75.86	-2.41
76.42	-2.01
81.81	-0.97

From Table 5.2, it can be seen that the developed noise cancellation algorithm consistently cancels the noise out from the FPCG even under conditions of increasing noise power. Post noise cancellation, the estimate $\hat{x}(n)$ was subjected to a six level MRA using fifth order Coiflet wavelet. The FHS and MHS were extracted as independent sources by performing a hard threshold on MRA coefficients, simultaneously retaining details and approximation coefficients of level six (D6 and

A6) and reconstructing them individually back into time domain. Figures 5.6.A1, 5.6.A2, 5.6.B1, 5.6.B2, 5.6.C1 and 5.6.C2 show the noisy signal with noise powers 73.12, 76.42, 81.81 dBs and the corresponding FHS and MHS signals obtained after MRA decomposition for six seconds of SNR enhanced FPCG, respectively.

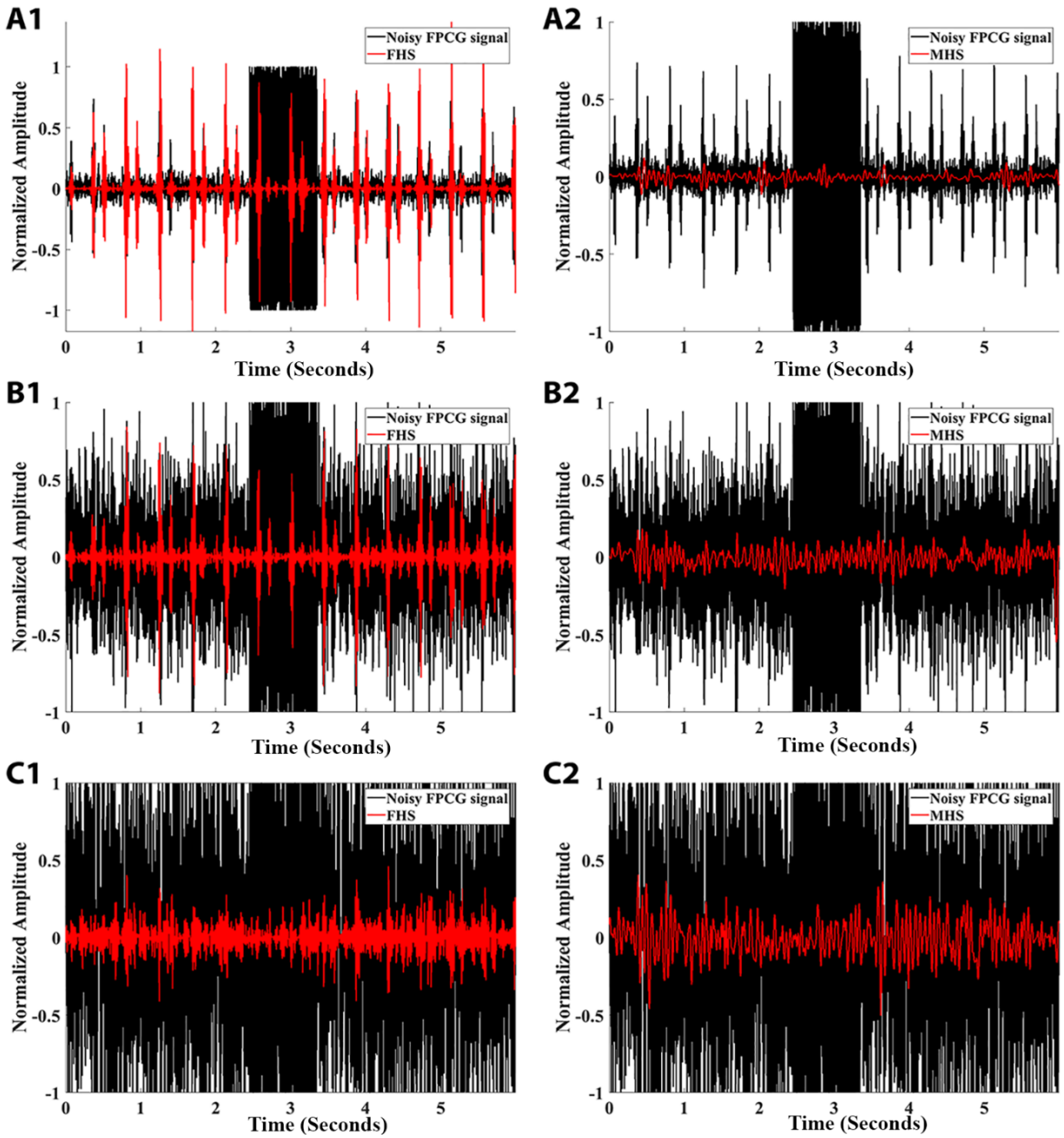

Figure 5.6: Noisy FPCG, Separated FHS and Separated MHS Corresponding to Various FPCG Noise Powers.

From Figures 5.6.A1 – 5.6.C2, it can be observed that, qualitatively the developed framework effectively attenuated the out-of-band noises and efficiently resolved the FHS and MHS interference from a single channel FPCG. However, in order to provide additional validation, mean Fetal and Maternal Heart Rates (FHR, MHR) along with their standard deviations (SD) were computed in beats per minute (bpm) for the analyzed FPCG dataset. Table 5.3 presents the results of the estimated FHR and MHR.

Table 5.3: Estimated FHR and MHR.

Standard Deviation of FPCG Noise (dB)	**FHR±SD (bpm)**	**MHR±SD (bpm)**
73.12	143±16	74±4
74.76	149±25	72±8
75.86	154±32	71±10
76.42	150±25	76±20
81.81	167±36	83±16

From Table 5.3, it can be seen that the estimated FHR and MHR fall within normal range, i.e., 110-210 bpm for FHS and 70-90 bpm for MHS [117].

CHAPTER 6: CONCLUSIONS AND FUTURE RESEARCH

6.1 Conclusions

Existing critical and emergency care blood flow based data acquisition systems are currently limited to only measuring continuous blood pressure. Inability to detect sensitive dynamic pressure variations and solve the problem of reducing external acoustic noise are the primary limiting factors. In addition, the use of multiple monitoring systems such as 12-lead electrocardiogram, capnogram, plethysmograph and Foley catheter present a plethora of other challenges including complex and expensive infrastructure, lack of functional interoperability and diagnostic precision in low resource settings. To address these challenges, a novel first of its kind, catheter multiscope was introduced in this research. The results of the proof of concept and the feasibility studies described in the dissertation show that the developed minimally invasive novel catheter multiscope can be used to measure critical parameters with clinical accuracy. In particular, the catheter multiscope is able to uniquely characterize a physiological phenomenon and continuously measure critical parameters such as: heart rate, respiratory rate, systolic pressure and diastolic pressure validated using small animal models. In comparison to the existing state-of-the-art, the developed technology exhibits innovation in terms of complexity of the data acquisition system, an efficient signal processing framework and an improved applicability for a low resource setting. The sensitive dynamic pressure variations within the blood flow were acquired using a data acquisition system that is a composed of a fluid coupled catheter, a fluid to air polymeric

membrane and an acoustic waveguide housing a pressure field microphone. Since the acquired dynamic pressure is severely affected due to other acoustic interferences present in critical and emergency care setting, its signal to noise ratio was improved by developing an efficient spectral subtraction based noise reduction algorithm. The performance assessment metrics such as noise factor and signal to noise ratio quantitatively validated that the developed algorithm provides a better performance compared to other state-of-the-art noise cancellation algorithms. Then, a wavelet based source separation algorithm was developed to separate various acoustic sources from a single channel observation. Using the novel source separation algorithm, acoustic heart and respiratory pulses were extracted from the noise reduced signal. The framework to process the acoustic signals of the novel catheter multiscope can be adapted to other single or multi-channel acoustic signals with minor or no modifications.

It was observed that there were no particular standards to validate the results of critical care data acquisition systems. Hence, in this dissertation, a procedure to validate and benchmark the performance of critical care data acquisition systems has been developed. The extracted acoustic heart and respiratory pulses were quantitatively validated by showing that the estimated average errors for the computed heart and respiratory rates were less than 15%. In addition, continuous blood pressure was derived from the measured total pressure by means of a novel signal processing framework. The derived systolic and diastolic pressures were quantitatively and qualitatively validated by benchmarking with the gold standard measurements and by establishing an additional benchmark with Physionet arterial blood pressure data. The estimated average errors for the computed systolic and diastolic pressures were less than 6%. Overall, the feasibility study shows that the developed novel catheter multiscope can provide multiple critical parameters like heart

rate, respiratory rate, systolic and diastolic pressures with clinical accuracy by measuring a physiological process.

In addition to demonstrating the feasibility of the developed catheter multiscope in critical and emergency care monitoring, the diagnostic potential of the developed technology has been shown in additional applications including sinus rhythm pattern recognition and fetal monitoring through phonocardiography. These application case studies are the byproducts of the catheter multiscope, i.e., similar or the same data acquisition system and signal processing framework have been utilized. The preliminary results show that it is feasible to measure multiple critical parameters from a single physiological phenomenon using the catheter multiscope. The methodology implemented in this research can be applied for research, development and optimization of other catheter based data acquisition systems for monitoring vital bio-signals. In conclusion, there is growing interest for disruptive technology like the catheter multiscope in the field of medical devices particularly, in critical and emergency care. It is the ultimate goal of this research to establish new frontiers in vital bio-signal monitoring for any critical and emergency care under any given low resource settings.

6.2 Future Research

From the current feasibility study, it was observed that various challenges with respect to the data acquisition system, data analysis and benchmarking have to be addressed in order to extract all the bio-signals of interest with fidelity.

6.2.1 Data Acquisition

With respect to the data acquisition system, the P_{static} was not measured with precision since the computed blood pressure waveform indicated the presence of distortions and resulted in an attenuated signal. The acoustic respiratory pulse was attenuated and presented as discontinuities

in the P_{total}. In order to address the challenges of the data acquisition system, P_{static} needs to be measured with a suitable pressure sensor. The frequency response of the P_{total} measuring sensor needs to be specified below 1 Hz to sense changes in the infrasonic sound pressures.

6.2.1.1 Future Design Optimizations

Though the pressure field microphone measures the dynamic pressures with high sensitivity and precision, it requires the use of a waveguide to effectively acquire the dynamic pressure. However, in order to comply with the regulations of FDA, the invasive/minimally invasive critical care data acquisition systems are only to be designed for one-time use. For these reasons, the use of waveguide and pressure field microphone make the data acquisition system expensive. Hence, future generation devices will have to be cost effective and designed for one-time use. Figure 6.1 shows the next generation design layout of the catheter multiscope that is capable of addressing the existing challenges.

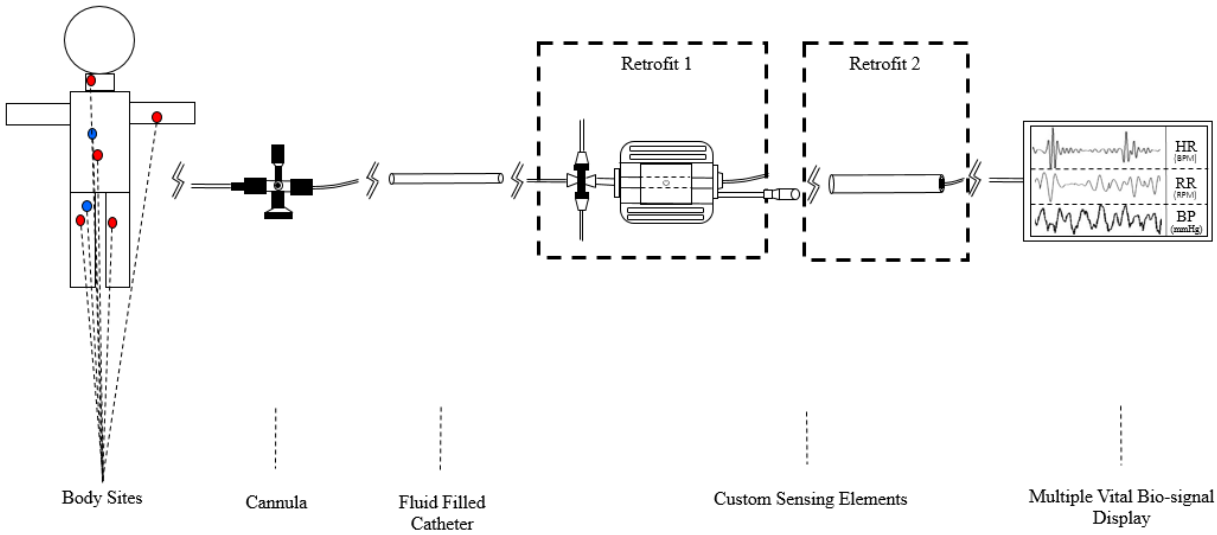

Figure 6.1: Next Generation Design Layout for Catheter Multiscope.

As shown in Figure 6.1, the existing data acquisition system will be retrofitted using retrofits 1 and 2. Retrofit 1 contains a MEMS based static pressure sensing element with a custom sensor housing designed to estimate fluid pressure. In addition, retrofit 1 also contains a custom

designed Y port, through which saline solution and other drugs can be infused. The Y port also enables expansion of the monitoring to other critical parameters such as SPO_2 and rapid blood analysis. Retrofit 2 contains a polymeric barrier that is used to provide fluid to air coupling and a MEMS microphone is fabricated on the barrier. This design of retrofit 2 eliminates the use of waveguide and pressure field microphone. In addition to optimizing the data acquisition system through retrofitting, computational fluid dynamics simulations will also be performed in future.

6.2.2 Data Collection and Signal Processing

With respect to data analysis, artifacts have not been processed and removed from the data and hence before performing any analysis, artifacts need to be attenuated. It should also be noted that this study did not consider evaluation metrics like mean squared error and computational efficiency in assessing the performance of the noise cancellation algorithms which is proposed for future research. Though MRA provided satisfactory bio-signal separation, the decomposition coefficients in the scales of interest had to be manually identified in the current study and hence it would be interesting to further process the MRA coefficients by an unsupervised clustering algorithm like K-means, Gaussian Mixture Models, etc. Though the acoustic heart pulses were extracted from the measured P_{total} without any distortion, it needs to be validated towards identification of pathology pertaining to the heart sounds. With respect to benchmarking, in the current study, additional modalities like respiratory rate and heart rate were noted prior and post data acquisition and hence in order to provide an accurate benchmarking these modalities need to be recorded electronically along with the P_{total} measurement. Also, the implemented blood pressure computation framework needs additional information from the conventional devices. Regarding continuous blood pressure, an accurate benchmark needs to be established in order to provide conclusive results and this is currently under study. Overall, the current data acquisition and

analysis were validated by acquiring vascular pressure measurements from small animal models which needs to be extended to humans.

6.2.3 Application Case Studies

6.2.3.1 Sinus Rhythm Pattern Recognition

Analysis presented in this dissertation evaluated the developed cluster analysis framework for the data collected from two different body sites. In order to validate the pattern recognition framework, the current case study needs to be implemented for data collected from more than two body sites and for various statically robust datasets collected from various animal studies. It should be noted that the segmentation accomplished prior feature extraction is a key cluster accuracy determining factor. In the current case study, the segmentation length has been chosen empirically and for the future study the segmentation needs to be defined based on the clustering objective. In order to improve currently obtained recognition accuracy of 94.37% for the developed framework, a multimodal framework has to be developed that includes information from other vital bio-signals of the catheter multiscope. Additionally, investigating multimodal features from blood pressure, acoustic heart and respiratory pulses may also contribute to the accuracy improvement. It is also worth noting that the current case study needs to be applied to various cases of pathological arrhythmia. Overall, the current data acquisition and cluster analysis framework was validated by acquiring vascular pressure measurements from a Yorkshire pig which needs to be extended to humans. The end goal is to be able to reduce the false arrhythmia alarm rates of the critical care units. In addition, the framework developed for the acoustic heart pulses of the catheter multiscope can also be extended and validated for classification of normal and abnormal heart sounds.

6.2.3.2 Fetal Monitoring Through Phonocardiography

Though the developed spectral subtraction algorithm was able to effectively remove the out-of-band noise, the noise factor was seen to be reducing across higher noise power ranges. Hence, in order to maintain consistent noise factor throughout all the power ranges of noise, the noise estimation algorithm within spectral subtraction will need to be improved in the future. In addition, a comparative analysis has to be performed with multiband spectral subtraction and other recent denoising techniques. In this application, the source separation algorithm was able to separate FHS and MHS from the simulated FPCG dataset. However, the proposed framework is currently being extended to a clinically collected FPCG dataset. Also, as a part of this analysis, the feasibility of separating additional vital bio-signals corresponding to the fetus and the mother is being assessed. FHR and MHR were manually computed for this case study and in the future this computation should be automated and validated against clinically collected cardiotocographs.

REFERENCES

[1] Centers for Disease Control and Prevention, "Emergency Department Visits," National Center for Health Statistics, 2017.

[2] J. Huygh, Y. Peeters, J. Bernards and M. Malbraina, "Hemodynamic Monitoring in the Critically Ill: An Overview of Current Cardiac Output Monitoring Methods," *F1000 Research,* vol. 5, no. 2855, pp. 1-9, 2016.

[3] L. Busse, D. Davison, C. Junker and L. Chawla, "Hemodynamic Monitoring in the Critical Care Environment," *Advances in Chronic Kidney Disease,* vol. 20, no. 1, pp. 21-29, 2013.

[4] E. Kipnis, D. Ramsingh, M. Bhargava, E. Dincer, M. Cannesson, A. Broccard, B. Vallet, K. Bendjelid and R. Thibault, "Monitoring in the Intensive Care," *Critical Care Research and Practice,* vol. 2012, pp. 1-20, 2012.

[5] C. Kuhn and K. Werdan, "Hemodynamic Monitoring," in *Surgical Treatment: Evidence-Based and Problem-Oriented,* Munich, W. Zuckschwerdt Verlag GmbH, 2001.

[6] S. Balaji, M. Ellenby, J. McNames and B. Goldstein, "Update on Intensive Care ECG and Cardiac Event Monitoring," *Cardiac Electrophysiology Review,* vol. 6, pp. 190-195, 2002.

[7] Z. Moussavim, Fundamentals of Respiratory Sounds and Analysis, Morgan & Claypool Publishers, 2006.

[8] R. Peura, "Blood Pressure And Sound," in *Medical Instrumentation Application and Design*, John Wiley & Sons, Inc., 2010, pp. 293 - 337.

[9] I. Moxham, "Physics of Invasive Blood Pressure Monitoring," *Southern African Journal of Anaesthesia and Analgesia,* vol. 9, no. 1, pp. 33 - 38, 2003.

[10] A. Van de Louw, C. Cracco, C. Cerf, A. Harf, P. Duvaldestin, P. Lemaire and L. Brochard, "Accuracy of Pulse Oximetry in Intensive Care Unit," *Intensive Care Medicine,* vol. 27, no. 10, pp. 1606 - 1613, 2001.

[11] J. Lefrant, L. Muller, J. Emmanuel, M. Benbabaali, C. Lebris, N. Zeitoun, C. Mari, G. Saïssi, J. Ripart and J. Eledjam, "Temperature Measurement in Intensive Care Patients: Comparison of Urinary Bladder, Oesophageal, Rectal, Axillary,and Inguinal Methods Versus Pulmonary Artery Core Method," *Intensive Care Medicine*, vol. 29, no. 3, pp. 414 - 418, 2003.

[12] Trauma and Life Support Center, "A Guide Patient For Patient and Family," 2015. [Online]. Available: https://www.uwhealth.org/healthfacts/trauma/4310.pdf.

[13] A. K. Abbas and R. Baseem, Phonocardiography Signal Processing, Morgan & Claypool Publishers, 2009.

[14] J. Allen, "Photoplethysmography and its Application in Clinical Physiological Measurement," *Physiological Measurement*, vol. 28, no. 3, pp. 1 - 39, 2007.

[15] M. Elgendi, "On the Analysis of Fingertip Photoplethysmogram Signals," *Current Cardiology Reviews*, vol. 8, no. 1, pp. 14-25, 2012.

[16] L. Brochard, G. Martin, L. Blanch, P. Pelosi, F. Belda, A. Jubran, L. Gattinoni, J. Mancebo, V. Ranieri, J. Richard, D. Gommers, A. Baron, A. Pesenti, S. Jaber, O. Stenqvist and J. Vincent, "Clinical Review: Respiratory Monitoring in the ICU - A Consensus of 16," *Critical Care*, vol. 16, no. 2, pp. 1- 14, 2012.

[17] M. De Georgia, F. Kaffashi, F. Jacono and K. Loparo, "Information Technology in Critical Care: Review of Monitoring and Data Acquisition Systems for Patient Care and Research," *The Scientific World Journal*, vol. 2015, pp. 1-9, 2015.

[18] D. Feigal, "Impact of the Regulatory Framework on Medical Device Development and Innovation," in *Public Health Effectiveness of the FDA 510(k) Clearance Process: Balancing Patient Safety and Innovation: Workshop Report*, Washington (DC), National Academy of Sciences, 2010, p. Appendix D.

[19] S. Hart, G. Dileo, A. Weitzenfeld, P. Hipol, M. Sweeney, F. Sinatra and K. Hufford, "Electronic Catheter Stethoscope". USA Patent US 20130018267A1, 17 September 2012.

[20] R. Sameni and G. Clifford, "A Review of Fetal ECG Signal Processing : Issues and Promising Directions," *US Natinal Library of Medicine*, no. 3, pp. 4 - 20, 2010.

[21] A. Ashley E and J. Niebauer, "Chapter 3, Conquering the ECG," in *Cardiology Explained*, London, Remedica, 2004.

[22] B. Goldstein, "Intensive Care Unit ECG Monitoring," *Cardiac Electrophysiology Review*, vol. 1, no. 3, pp. 308-310, 1997.

[23] D. Poulikakos and M. Malik, "Challenges of ECG Monitoring and ECG Interpretation in Dialysis Units," *Journal of Electrocardiology,* vol. 49, no. 6, pp. 855-859, 2016.

[24] M. Broszko and C. Stanciu, "Survey of EKG Monitoring Practices: A Necessity or Prolonged Nuisance?," *The American Journal of Psychiatry Residents' Journal,* vol. 12, no. 3, pp. 6-9, 2017.

[25] A. Goldberger, L. Amaral, L. Glass, J. Hausdorff, C. Ivanov P, R. Mark, J. Mietus, G. Moody, C. Peng and H. Stanley, "Components of a New Research Resource for Complex Physiologic Signals," *PhysioBank, PhysioToolkit, and PhysioNet,* vol. 101, no. 23, pp. e215-e220, 2000.

[26] X. Ding, N. Zhao, G. Yang, R. Pettigrew, B. Lo, F. Miao, Y. Li, J. Liu and Y. Zhang, "Continuous Blood Pressure Measurement From Invasive to Unobtrusive: Celebration of 200th Birth Anniversary of Carl Ludwig," *IEEE Journal Of Biomedical And Health Informatics,* vol. 20, no. 6, pp. 1455-1465, 2016.

[27] J. Webster, The Measurement, Instrumentation and Sensors Handbook, Boca Raton: CRC Press, 1999.

[28] S. Esper and M. Pinsky, "Arterial Waveform Analysis," *Best Practice & Research Clinical Anaesthesiology,* vol. 28, pp. 363-380, 2014.

[29] B. McGhee and M. Bridges, "Monitoring Arterial Blood Pressure: What You May Not Know," *Critical Care Nurse,* vol. 22, no. 2, pp. 60-79, 2002.

[30] M. Reems and M. Aumann, "Central Venous Pressure: Principles, Measurement and Interpretation," Vetstreet Inc., 2012.

[31] U. Gidwani, B. Mohanty and K. Chatterjee, "The Pulmonary Artery Catheter: A Critical Reappraisal," *Cardiology Clinics,* vol. 31, no. 4, pp. 545-565, 2013.

[32] M. Hadian and M. Pinsky, "Evidence-Based Review of the Use of the Pulmonary Artery Catheter: Impact Data and Complications," *Critical Care,* vol. 10, no. 3, pp. 1-11, 2006.

[33] T. Sugimoto, K. Dohi, M. Tanabe, K. Watanabe, E. Sugiura, S. Nakamori, T. Yamada, K. Onishi, M. Nakamura, T. Nobori and M. Ito, "Echocardiographic Estimation of Pulmonary Capillary Wedge Pressure Using the Combination of Diastolic Annular and Mitral Inflow Velocities," *Journal of Echocardiography,* vol. 11, no. 1, pp. 1-8, 2013.

[34] M. Pozzoli, S. Capomolla, G. Pinna, F. Cobelli and L. Tavazzi, "Doppler Echocardiography Reliably Predicts Pulmonary Artery Wedge Pressure in Patients with Chronic Heart Failure With and Without Mitral Regurgitation," *Journal of the American College of Cardiology,* vol. 27, no. 4, pp. 883-893, 1996.

[35] J. Vanoverschelde, A. Robert, A. Gerbaux, X. Michel, C. Hanet and W. Wiins, "Noninvasive Estimation of Pulmonary Arterial Wedge Pressure With Doppler l'ransmitral Flow Velocity Pattern in Patients With Known Heart Disease," *The American Journal Of Cardiology,* vol. 75, no. 5, pp. 383-389, 1995.

[36] J. Welch, P. Ford, R. Teplick and R. Rubsamen, "The Massachusetts General Hospital-Marquette Foundation Hemodynamic and Electrocardiographic Database - Comprehensive collection of critical care waveforms," *Journal of Clinical Monitoring,* vol. 7, no. 1, pp. 96-97, 1991.

[37] S. Nadeau and W. Noble, "Limitations of Cardiac Output Measurements by Thermodilution," *Canadian Anaesthetists Society Journal,* vol. 33, no. 6, p. 780–784, 1986.

[38] J. Huygh, Y. Peeters, J. Bernards and M. Malbrain, "Hemodynamic Monitoring in the Critically Ill: An Overview of Current Cardiac Output Monitoring Methods," *F1000 Research,* vol. 5, no. 2855, pp. 1-9, 2016.

[39] S. Tibby and I. Murdoch, "Monitoring Cardiac Function in Intensive Care," *Archives of Disease in Childhood,* vol. 88, no. 1, pp. 46-52, 2003.

[40] I. Kerslake and F. Kelly, "Uses of Capnography in the Critical Care Unit," *British Journal of Anaesthesia,* vol. 17, no. 5, p. 178–183, 2016.

[41] P. Theerawit, Y. Sutherasan, L. Ball and P. Pelosi, "Respiratory Monitoring in Adult Intensive Care Unit," *Expert Review of Respiratory Medicine,* vol. 11, no. 6, pp. 453-468, 2017.

[42] C. Anderson and P. Breen, "Carbon Dioxide Kinetics and Capnography During Critical Care," *Critical Care,* vol. 4, no. 4, pp. 207-215, 2000.

[43] N. Mandal, "Respirometers Including Spirometer, Pneumotachograph and Peak Flow Meter," *Anaesthesia & Intensive Care Medicine,* vol. 7, no. 1, pp. 1-5, 2006.

[44] J. Toffaletti and C. Rackley, "Advances in Clinical Chemistry," in *Chapter Three - Monitoring Oxygen Status*, Elsevier, 2016, pp. 103-124.

[45] "Photoplethysmography and its Application in Clinical Physiological Measurement," *Physiological Measurement,* vol. 28, no. 3, pp. R1-R37, 2007.

[46] M. Delost, "Blood Gas and Critical Care Analyte Analysis," in *Equipment for Respiratory Care*, Jones & Bartlett, 2016, pp. 151-174.

[47] Y. Budak, K. Huysal and M. Polat, "Use of a Blood Gas Analyzer and a Laboratory Autoanalyzer in Routine Practice to Measure Electrolytes in Intensive Care Unit Patients," *BMC Anesthesiology,* pp. 12-17, 2012.

[48] R. Pearse and A. Rhodes, "Mixed and Central Venous Oxygen Saturation," pp. 592-602.

[49] T. Koo, *Measurement of Blood Analytes in Turbid Biological Tissue Using Near-infrared Raman Spectroscopy*, Massachusetts: Massachusetts Institute of Technology, 2001.

[50] A. Draghici and A. Taylor, "The Physiological Basis and Measurement of Heart Rate Variability in Humans," *Journal of Physiological Anthropology*, vol. 35, no. 22, pp. 1-8, 2016.

[51] C. Julien, "The Enigma of Mayer Waves: Facts and Models," *Cardiovascular Research*, vol. 70, no. 1, pp. 12-21, 2006.

[52] Y. Harati and S. Izadyar, "Chapter 12 – Autonomic Nervous System," in *Neurology Secrets*, Philadelphia, Mosby Inc., 2010, p. 204–226.

[53] G. Bishop, K. Shigemi, J. Freeman and M. Brunner, "Baroreflex Control of Arterial and Venous Compliances and Vascular Capacity in Hypertensive Dogs," *American Journal of Physiology*, vol. 265, no. 1, pp. H96-H102, 1993.

[54] A. Radaelli, R. Raco, P. Perfetti, A. Viola, A. Azzellino, M. Signorini and A. Ferrari, "Effects of Slow, Controlled Breathing on Baroreceptor Control of Heart Rate and Blood Pressure in Healthy Men," *Journal of Hypertension*, vol. 22, no. 7, p. 1361–1370, 2004.

[55] T. Lewis, "Studies of the Relationship Between Respiration and Blood-pressure," *The Journal of physiology*, vol. 37, no. 3, p. 213–232, 1908.

[56] L. Bernardi, C. Porta, A. Gabutti, L. Spicuzza and P. Sleight, "Modulatory Effects of Respiration," *Autonomic Neuroscience*, vol. 90, no. 1, p. 47–56, 2001.

[57] N. Selvaraj, A. Jaryal, J. Santhosh, K. Deepak and S. Anand, "Influence of Respiratory Rate on the Variability of Blood Volume Pulse Characteristics," *Journal of Medical Engineering and Technology*, vol. 35, no. 5, p. 370–375, 2009.

[58] V. Novak, P. Novak, J. De Champlain, A. Le Blanc, R. Martin and R. Nadeau, "Influence of Respiration on Heart Rate and Blood Pressure," *Journal of Applied Physiology*, vol. 74, no. 2, p. 617–626, 1993.

[59] C. Caro, T. Pedley, R. Schroter and W. Seed, The Mechanics of the Circulation, Cambridge: Cambridge University Press, 2012.

[60] G.R.A.S. Sound & Vibration, "G.R.A.S. 46AD 1/2" CCP Pressure Standard Microphone Set," G.R.A.S. Sound & Vibration, 2016. [Online]. Available: http://www.gras.dk/46ad.html. [Accessed 20 January 2017].

[61] G.R.A.S. Sound & Vibration, "G.R.A.S. 46AE 1/2" CCP Free-field Standard Microphone Set," G.R.A.S. Sound & Vibration, 2016. [Online]. Available: http://www.gras.dk/46ae.html. [Accessed 20 January 2017].

[62] National Instruments, "NI 446x Specifications," National Instruments, 2017. [Online]. Available: http://www.ni.com/pdf/manuals/373770j.pdf. [Accessed 20 January 2017].

[63] Y. Cengel and J. Cimbala, Fluid Mechnanics: Fundamentals and Applications, New York: The McGraw-Hill Companies,Inc., 2014.

[64] E. Frederiksen, "Acoustic Metrology – An Overview of Calibration Methods and Their Uncertainties," *International Iournal of Metrology and Quality Engineering*, vol. 4, no. 2, pp. 97-107, 2013.

[65] Bruel & Kjaer, "Measurement Microphones," 1994. [Online]. Available: https://www.bksv.com/media/doc/br0567.pdf.

[66] J. Poruba, "Speech Enhancement Based On Nonlinear Spectral Subtraction," in *IEEE International Caracas Conference on Devices, Circuits and Systems.*, Aruba, 2002.

[67] R. Udrea and S. Ciochinri, "Speech Enhancement Using Spectral Oversubtraction And Residual Noise Reduction," in *International Symposium on Signals, Circuits and Systems*, lasi, Romania, 2003.

[68] M. Okazaki, T. Kunimoto and T. Kobayashi, "Multi-Stage Spectral Subtraction For Enhancement Of Audio Signals," in *IEEE International Conference on Acoustics, Speech, and Signal Processing*, Montreal, Canada, 2004.

[69] S. Takada, S. Kanba, T. Ogawa, K. Akagiri and T. Kobayashi, "Sound Source Separation Using Null-Beamforming And Spectral Subtraction For Mobile Devices," in *IEEE Workshop on Applications of Signal Processing to Audio and Acoustics*, New Paltz, NY, 2007.

[70] T. Tosanguan, R. Dickinson and E. Drakakis, "Modified Spectral Subtraction For De-noising Heart Sounds: Interference Suppression via Spectral Comparison," in *IEEE Biomedical Circuits and Systems Conference*, Baltimore,MD, 2008.

[71] S. V. Vaseghi, Advanced Signal processing and Digital Noise Reduction, NY: John Wiley & Sons, Inc.,, 1996.

[72] S. Haykin, "Frquency - Domain Adaptive Filters," in *Adaptive Filter Theory*, New Jersey, Prentice Hall, Inc., 1996, pp. 445 - 478.

[73] K. Hashiodani, T. Onoue, S. Takada, Y. Fukumizu and Y. Yamauchi, "Biosignals Separation Method For Medical Diagnostic System," in *5th International Symposium On Medical Information & Communication Technology (ISMICT)*, Switzerland, 2011.

[74] D. Flores-Tapia, Z. Moussavi and G. Thomas, "Heart Sound Cancellation Based on Multiscale Products and Linear Prediction," *IEEE Transaction On Biomedical Engineering*, vol. 54, no. 2, pp. 234 - 243, 2007.

[75] F. Jin, F. Sattar, S. Razul and D. Goh, "Heart Sound Localization From Respiratory Sound Using A Robust Wavelet Based Approach," in *IEEE International Conference on Multimedia and Expo*, Hannover, Germany, 2008.

[76] D. Percival and A. Walden, Wavelet Methods for Time Series Analysis, Cambridge: Cambridge University Press, 2000.

[77] A. Shcherbina, C. M. Mattsson, D. Waggott, H. Salisbury, J. W. Christle, T. Hastie, M. T. Wheeler and E. A. Ashley, "Accuracy in Wrist-Worn, Sensor-Based Measurements of Heart Rate and Energy Expenditure in a Diverse Cohort," *Journal of Personalized Medicine*, vol. 7, no. 3, p. 19, 2017.

[78] W. Karlen, H. Gan, M. Chiu, D. Dunsmuir, G. Zhou, G. A. Dumont and J. M. Ansermino, "Improving the Accuracy and Efficiency of Respiratory Rate Measurements in Children Using Mobile Devices," *PLoS One*, vol. 9, no. 6, pp. 1- 9, 2014.

[79] National Center for Chronic Disease Prevention and Health Promotion, Division for Heart Disease and Stroke Prevention, "Heart Disease Facts," Centers for Disease Control and Prevention, 2015.

[80] G. Clifford, I. Silva, B. Moody, Q. Li, D. Kella, A. Chahin, T. Kooistra, D. Perry and R. Mark, "False Alarm Reduction in Critical Care," *Journal of Physiological Measurement*, vol. 37, no. 8, pp. E5 - E23, 2016.

[81] S. C. Burrus, R. Gopinath and G. Haitao, Introduction to Wavelets and Wavelet Transform, New Jersey: Prentice-Hall, 1998.

[82] B. Christopher, Pattern Recognition and Machine Learning, Singapore: Springer, 2006.

[83] P. Rousseeuw, "Silhouettes: A Graphical Aid to the Interpretation and Validation of Cluster Analysis," *Journal of Computational and Applied Mathematics*, vol. 20, pp. 53 - 65, 1986.

[84] F. Marian and C. Elizabeth, "Fetal and Perinatal Mortality: United States, 2013," *National Vital*, vol. 54, no. 8, pp. 1 - 24, 2015.

[85] WHEC Practice Bulletin and Clinical Management Guidelines for healthcare providers., "Intrapartum Electronic Fetal Monitoring," Women's Health and Education Center (WHEC), 11 December 2009. [Online]. Available: http://www.womenshealthsection.com/content/obs/obs028.php3.

[86] A. M. Ioyce, E. Brady, J. Michelle and C. Sally, "Births : Final Data for 2012," National Vital Statistics Report, U.S. Department of Health and Human Services, 2013.

[87] D. Ayres-de-Campos and J. Bernardes, "Twenty- Five Years after the FIGO Guidelines for the Use of Fetal Monitoring: Time for a Simplified Approach ?," *International Journal of Gynecology & Obstetrics*, vol. 110, no. 1, pp. 1 - 6, 2010.

[88] A. David and A. Lisa, "Electronic Fetal Heart Rate Monitoring : Applying Principles of Patient Safety," *American Journal of Obstetrics & Gynecology*, p. 6, 2012.

[89] P. Thomas, "Electronic Fetal Monitoring : A Bridge Too Far," *The Journal of Legal Medicine*, vol. 33, p. 72, 2012.

[90] E. Kennedy, Observations on Obstetric Auscultations, Dublin , Ireland: Hodges and Smith, 1833.

[91] A. Cook, R. Yates and R. H. Anderson, "Normal and Abnormal Fetal Cardiac Anatomy," in *Prenatal Diagnosis*, John Wiley & Sons, Ltd., 2004, p. 1032–1048.

[92] M. Anisha, S. Kumar and M. Benisha, "Survey on Fetal ECG Extraction," in *International Conference on Control, Instrumentation, Communication and Computational Technologies (ICCICCT)*, Kanyakumari,India, 2014.

[93] J. G. Stinstra, "The Reliability of Fetal Magnetocardiogram," Twente University Press, Netherlands, 2001.

[94] E. Zahedi and G. Beng, "Applicability of Adaptive Noise Cancellation to Fetal Heart Rate Detection Using Photoplethysmography," *Computers in Biology and Medicine*, vol. 38, no. 1, pp. 31 - 41, 2008.

[95] T. Euliano, M. Nguyen, S. Darmanjian, S. Mcgorry, N. Euliano, A. Onkala and A. Gregg, "Monitoring Uterine Activity During Labor: A Comparison of Three Methods," *American Journal of Obstetrics and Gynecology*, vol. 208, no. 1, pp. 66.e1 - 66. e6, 2013.

[96] The American Institute of Ultrasound in Medicine, "AIUM Practice Guidelines for the Performance of Fetal Echocardiography," *Journal of ultrasound in medicine: official journal of the American Institute*, vol. 32, no. 6, pp. 1067 - 1082, 2013.

[97] Z. Alfirevic, D. Devane and G. Gyte, "Continuous Cardiotocography as a Form of Electronic Fetal Monitoring For Fetal Assessment During Labour (Review)," *Cochrane Database of Systematic Reviews,* vol. CD006066, no. 5, 2013.

[98] A. Zukerwar, R. Pretlow, J. Stoughton and D. A. Baker, "Development of a Piezoploymer Pressure Sensor for a Portable Fetal Heart Rate Monitor," *IEEE Transacations on Biomedical Engineering,* vol. 40, no. 9, pp. 963 - 969, 1993.

[99] S. Noorzadeh, "Extraction of Fetal ECG and its Characteristics Using Multi-modality," Universite Grenoble Alpes, France, 2015.

[100] M. Hasan, M. B. I. Reaz, M. I. Ibrahimy, M. Hussain and J. Uddin, "Detection and Processing Techniques of FECG Signal for Fetal Monitoring," *Biological Procedures Online,* vol. 11, no. 1, pp. 263-295, 2009.

[101] J. Nagel, "New Diagnostic and Technical Aspects of Fetal Phonocardiography," *Science Direct,* vol. 23, p. 9, 1986.

[102] M. Pena, R. Gonzalez, T. Aljama, S. Carrasco, R. Ortiz and V. Valencia, "Comparision of Abdominal Ecg and Phonocardiography for Instantaneous Fetal Heart Rate Detection," in *17th Annual Conference of IEEE Engineering in Medicine and Biology Society,* Chicago, 1997.

[103] M. Godinez, A. Jimnez, R. Ortiz and M. Pena, "Online Fetal Heart Rate Monitor by Phonocardiography," in *IEEE*, Cancun,Mexico, 2003.

[104] P. C. A. M. Bakker, G. J. Colenbrander, A. A. Verstraeten and H. Van Geijn, "The Quality of Intrapartum Fetal Heart Rate Monitoring," *European Journal of Obstetrics & Gynecology and Reproductive Biology,* vol. 116, no. 1, pp. 22-27, 2004.

[105] J. MacDonnell, "Knowledge Based Interpretation of Fetal Phonocardiographic Signals," in *Transactions of the IEEE*, 1990.

[106] S. Barnett and D. Maulik, "Guidelines and Recommendations For Safe Use of Doppler Ultrasound in Perinatal Applications," *Journal of Maternal-Fetal and Neonatal Medicine*, vol. 10, no. 2, p. 75–84, 2001.

[107] H. Kieler, S. Cnattingiust, B. Haglund, J. Palmgren and O. Axelsson, "Ultrasound and Adverse Effects," *Ultrasound in Obstetrics and Gynecology,* vol. 20, no. 1, pp. 102-103, 2002.

[108] M. Ibrahimy, F. Ahmed, M. Ali and E. Zahedi, "Real-time Signal Processing for Fetal Heart Rate Monitoring," *IEEE Transactions on Biomedical Engineering* , vol. 50, no. 2, pp. 258 - 261, 2003.

[109] E. Ang, V. Gluncic, A. Duque, M. Schafer and P. Rakic, "Prenatal Exposure to Ultrasound Waves Impacts Neuronal Migration in Mice," *Proceedings of the National Academy of Sciences,* vol. 103, no. 34, pp. 12903-12910, 2006.

[110] J. Abramowicz, "Prenatal Exposure to Ultrasound Waves: Is There a Risk?," *Ultrasound in Obstetrics and Gynecology,* vol. 29, no. 10, p. 363–367, 2007.

[111] M. Ruffo, A. McEwan, A. Van Schaik, C. Sullivan, C. Jin, G. Gargiulo, M. Romano, M. Cesarelli, P. Bifulco and R. W. Shephard, "Non Invasive Foetal Monitoring with a Combined ECG-PCG System," INTECH Open Access Publisher, 2011.

[112] Y. Song, W. Xie, J. Chen and K. Phua, "Passive Acoustic Maternal Abdominal Fetal Heart Rate Monitoring Using Wavelet Transform," in *IEEE Computers in Cardiology*, Valencia, 2006.

[113] J. Chen, K. Phua, Y. Song and L. Shue, "A Portable Phonocardiographic Fetal Heart Rate Monitor," in *IEEE International Symposium on Circuits and Systems* , Greece, 2006.

[114] A. Jimenez, M. Ortiz, M. Pena, S. Charleston, R. Gonzalez, A. Aljama and S. Cmasco, "Performance of a Method to Generate Fetal Cardiotachograms Using Fetal Phonocardiography," in *IEEE Computer in Cardiology*, Rotterdam,Netherlands, 2001.

[115] E. Abdulhay, R. Oweis, M. Alhaddad, N. Sublaban, A. Radwan and H. Almasaeed, "Review Article: Non-Invasive Fetal Heart Rate Monitoring Techniques," *Biomedical Science and Engineering,* vol. 2, no. 3, pp. 53 - 67, 2014.

[116] T. Balaji, C. Anirudh, R. Abhinav, J. Prashant and B. Neerja, "Fetomaternal Parameter Monitoring System". Patent WO2015082987 A1, 11 June 2015.

[117] P. Chetlur Adithya, R. Sankar, W. Moreno and S. Hart, "Trends in Fetal Monitoring Through Phonocardiography: Challenges and Future Directions," *Biomedical Signal Processing and Control,* vol. 33, pp. 289-305, 2017.

[118] M. Cesarelli, M. Ruffo, M. Romano and P. Bifulco, "Simulation of Foetal Phonocardiographic Recordings for Testing of FHR Extraction Algorithms," *Computer Methods and Programs in Biomedicine,* vol. I, no. 07, pp. 513 - 523, 2012.

[119] A. Ericsson, M. Crim and C. Franklin, "A Brief History of Animal Modeling," *Journal of the Missouri State Medical Association,* vol. 110, no. 3, pp. 201-205, 2013.

[120] J. Welch, P. Ford, R. Teplick and R. Rubsamen, "The Massachusetts General Hospital-Marquette Foundation Hemodynamic and Electrocardiographic Database -- Comprehensive collection of critical care waveforms," *Journal of Clinical Monitoring,* vol. 7, no. 1, pp. 96 - 97, 1991.

[121] P. Chetlur Adithya, R. Sankar, W. Moreno and S. Hart, "A Novel Acoustic Catheter Stethoscope Based Acquisition and Signal Processing Framework to Extract Multiple Bio Signals," in *IEEE Engineering in Medicine and Biology Society* , Jeju Island, Korea, 2017.

[122] P. Chetlur Adithya, R. Sankar, W. Moreno and S. Hart, "A Novel Acquisition and Signal Processing Framework to Unmask Multiple Vital Bio Signals". US Provisional Patent 62/454,507, 3 February 2017.

[123] P. Chetlur Adithya, R. Sankar, W. Moreno and S. Hart, "Systems And Methods For Determining Physiological Parameters From Blood Flow Dynamics". US Utility Patent 15/888,889, 5 February 2018.

[124] P. Chetlur Adithya, S. Pandey, R. Sankar, S. Hart and W. Moreno, "Cluster Analysis Framework for Novel Acoustic Catheter Stethoscope," in *NIH - IEEE Special Topics Conference on Healthcare Innovations and Point of Care Technologies: Technology in Translation*, Baltimore, MD, 2017.

[125] P. Chetlur Adithya, S. Pandey, R. Sankar, W. Moreno, S. Hart and I. Ra, "Bio Acoustic Signal Feature Extraction and Pattern Recognistion Framework," in *International Conference on Software & Smart Convergence*, Vladivostok, Russia, 2017.

[126] P. Chelur Adithya, R. Sankar, W. Moreno, M. Cain, S. Hart, M. Simoes and C. Reyes, "Fetal Monitoring through Phonocardiography," in *IEEE Engineering in Medicine and Biology Society*, Chicago, 2014.

APPENDIX A: ADDITIONAL VALIDATION FOR NORMALIZED BLOOD PRESSURE

For additional validation of normalized blood pressure data extracted from the novel catheter multiscope, a frequency domain benchmarking was also performed with human blood pressure. The rationale behind establishing comparison between the human and animal blood pressure comes from the fact that specific animal models, particularly porcine and human physiological data share similar characteristics [119]. Figure A.1(a) shows the normalized continuous blood pressure computed from the catheter multiscope's measurement and Figure A.1(b) shows the arterial blood pressure data extracted from the PhysioNet waveform multi-parameter database [120, 25] over a period of ten seconds.

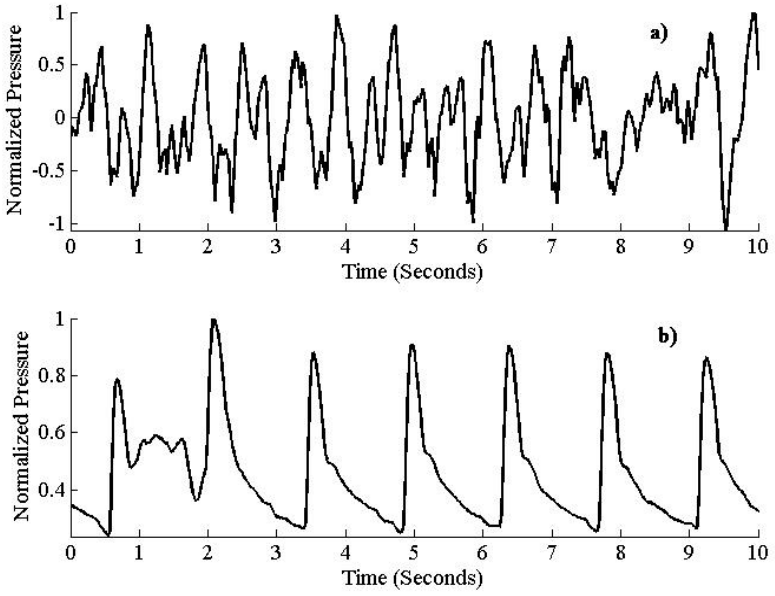

Figure A.1: Normalized Blood Pressure of Catheter Multiscope and Arterial Blood Pressure from the PhysioNet Database.

This benchmarking was accomplished by estimating the magnitude squared coherence between the blood pressure data derived from recording index 1a and the Physionet arterial blood pressure using Welch's overlapped segment averaging method with 5 second long frames and 75% overlap. Figure A.2 presents the results of estimated magnitude squared coherence.

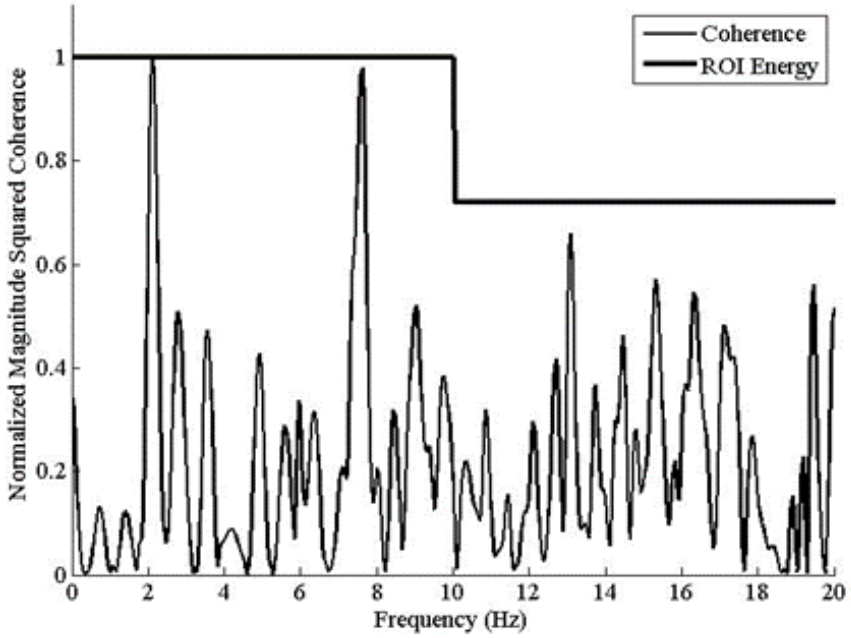

Figure A.2: Estimated Magnitude Squared Coherence.

It was observed that the magnitude squared coherence was dominant particularly around 2 Hz and 7 Hz. The Region of Interest (ROI) energy was estimated by computing the energy of the normalized magnitude squared coherence over 0 – 10 Hz and 10 – 20 Hz frequency bands. The ROI energy indicated that the derived blood pressure and Physionet blood pressure were significantly correlated over a frequency band of 0 – 10 Hz. The additional blood pressure validation results presented for the recording index 1a, shown in Figure A.2 is also applicable to other recording indices described in Table 3.1.

APPENDIX B: COPYRIGHT PERMISSIONS

B.1 IACUC Certificate for Animal Study

RESEARCH INTEGRITY AND COMPLIANCE
INSTITUTIONAL ANIMAL CARE & USE COMMITTEE

MEMORANDUM

TO:	Stuart Hart, M.D.
FROM:	Farah Moulvi, MSPH, IACUC Coordinator Institutional Animal Care & Use Committee Research Integrity & Compliance
DATE:	12/7/2015
PROJECT TITLE:	eCath
FUNDING SOURCE:	USF department, institute, center, etc.
IACUC PROTOCOL #:	R IS00001865
PROTOCOL STATUS:	**APPROVED**

The Institutional Animal Care and Use Committee (IACUC) reviewed your application requesting the use of animals in research for the above-entitled study. The IACUC **APPROVED** your request to use the following animals in your **protocol for a one-year period beginning 12/7/2015:**

Pig: Yorkshire (30-70kg male or female)	20

Please take note of the following:

• **IACUC approval is granted for a one-year period at the end of which, an annual renewal form must be submitted for years two (2) and three (3) of the protocol through the eIACUC system.** After three years all continuing studies must be completely re-described in a new electronic application and submitted to IACUC for review.

• **All modifications to the IACUC-Approved Protocol must be approved by the IACUC prior to initiating the modification.** Modifications can be submitted to the IACUC for review and approval as an Amendment or Procedural Change through the eIACUC system. These changes must be within the scope of the original research hypothesis, involve the original species and justified in writing. Any change in the IACUC-approved protocol that does not meet the latter definition is considered a major protocol change and requires the submission of a new application.

• **All costs invoiced to a grant account must be allocable to the purpose of the grant.** Costs allocable to one protocol may not be shifted to another in order to meet deficiencies caused by overruns, or for other reasons convenience. Rotation of charges among protocols by month without establishing that the rotation schedule credibly reflects the relative benefit to each protocol is unacceptable.

RESEARCH & INNOVATION • RESEARCH INTEGRITY AND COMPLIANCE
INSTITUTIONAL ANIMAL CARE AND USE COMMITTEE
PHS No. A4100-01, AAALAC No. 000434, USDA No. 58-R-0015
University of South Florida • 12901 Bruce B. Downs Blvd., MDC35 • Tampa, FL 33612-4799
(813) 974-7106 • FAX (813) 974-7091

B.2 Permission to Use Published Content in Chapters 3 and 4

3/27/2018 RightsLink® by Copyright Clearance Center

Copyright Clearance Center RightsLink®

Home | Create Account | Help

IEEE Requesting permission to reuse content from an IEEE publication

Title:	A novel acoustic catheter stethoscope based acquisition and signal processing framework to extract multiple bio signals
Conference Proceedings:	Engineering in Medicine and Biology Society (EMBC), 2017 39th Annual International Conference of the IEEE
Author:	Prashanth Chetlur Adithya
Publisher:	IEEE
Date:	July 2017

Copyright © 2017, IEEE

LOGIN

If you're a copyright.com user, you can login to RightsLink using your copyright.com credentials.

Already a RightsLink user or want to learn more?

Thesis / Dissertation Reuse

The IEEE does not require individuals working on a thesis to obtain a formal reuse license, however, you may print out this statement to be used as a permission grant:

Requirements to be followed when using any portion (e.g., figure, graph, table, or textual material) of an IEEE copyrighted paper in a thesis:

1) In the case of textual material (e.g., using short quotes or referring to the work within these papers) users must give full credit to the original source (author, paper, publication) followed by the IEEE copyright line © 2011 IEEE.
2) In the case of illustrations or tabular material, we require that the copyright line © [Year of original publication] IEEE appear prominently with each reprinted figure and/or table.
3) If a substantial portion of the original paper is to be used, and if you are not the senior author, also obtain the senior author's approval.

Requirements to be followed when using an entire IEEE copyrighted paper in a thesis:

1) The following IEEE copyright/ credit notice should be placed prominently in the references: © [year of original publication] IEEE. Reprinted, with permission, from [author names, paper title, IEEE publication title, and month/year of publication]
2) Only the accepted version of an IEEE copyrighted paper can be used when posting the paper or your thesis on-line.
3) In placing the thesis on the author's university website, please display the following message in a prominent place on the website: In reference to IEEE copyrighted material which is used with permission in this thesis, the IEEE does not endorse any of [university/educational entity's name goes here]'s products or services. Internal or personal use of this material is permitted. If interested in reprinting/republishing IEEE copyrighted material for advertising or promotional purposes or for creating new collective works for resale or redistribution, please go to http://www.ieee.org/publications_standards/publications/rights/rights_link.html to learn how to obtain a License from RightsLink.

If applicable, University Microfilms and/or ProQuest Library, or the Archives of Canada may supply single copies of the dissertation.

BACK | CLOSE WINDOW

Copyright © 2018 Copyright Clearance Center, Inc. All Rights Reserved. Privacy statement. Terms and Conditions.
Comments? We would like to hear from you. E-mail us at customercare@copyright.com

B.3 Permission to Use Published Content in Chapter 5, Section 5.1

3/27/2018 RightsLink® by Copyright Clearance Center

Copyright Clearance Center RightsLink®

Home | Create Account | Help

IEEE Requesting permission to reuse content from an IEEE publication

Title:	Cluster analysis framework for novel acoustic catheter stethoscope
Conference Proceedings:	Healthcare Innovations and Point of Care Technologies (HI-POCT), 2017 IEEE
Author:	Prashanth Chetlur Adithya
Publisher:	IEEE
Date:	Nov. 2017

Copyright © 2017, IEEE

LOGIN

If you're a copyright.com user, you can login to RightsLink using your copyright.com credentials.

Already a RightsLink user or want to learn more?

Thesis / Dissertation Reuse

The IEEE does not require individuals working on a thesis to obtain a formal reuse license, however, you may print out this statement to be used as a permission grant:

Requirements to be followed when using any portion (e.g., figure, graph, table, or textual material) of an IEEE copyrighted paper in a thesis:

1) In the case of textual material (e.g., using short quotes or referring to the work within these papers) users must give full credit to the original source (author, paper, publication) followed by the IEEE copyright line © 2011 IEEE.
2) In the case of illustrations or tabular material, we require that the copyright line © [Year of original publication] IEEE appear prominently with each reprinted figure and/or table.
3) If a substantial portion of the original paper is to be used, and if you are not the senior author, also obtain the senior author's approval.

Requirements to be followed when using an entire IEEE copyrighted paper in a thesis:

1) The following IEEE copyright/ credit notice should be placed prominently in the references: © [year of original publication] IEEE. Reprinted, with permission, from [author names, paper title, IEEE publication title, and month/year of publication]
2) Only the accepted version of an IEEE copyrighted paper can be used when posting the paper or your thesis on-line.
3) In placing the thesis on the author's university website, please display the following message in a prominent place on the website: In reference to IEEE copyrighted material which is used with permission in this thesis, the IEEE does not endorse any of [university/educational entity's name goes here]'s products or services. Internal or personal use of this material is permitted. If interested in reprinting/republishing IEEE copyrighted material for advertising or promotional purposes or for creating new collective works for resale or redistribution, please go to http://www.ieee.org/publications_standards/publications/rights/rights_link.html to learn how to obtain a License from RightsLink.

If applicable, University Microfilms and/or ProQuest Library, or the Archives of Canada may supply single copies of the dissertation.

BACK | CLOSE WINDOW

Copyright © 2018 Copyright Clearance Center, Inc. All Rights Reserved. Privacy statement. Terms and Conditions.
Comments? We would like to hear from you. E-mail us at customercare@copyright.com

B.4 Permission to Use Published Content in Chapter 5, Section 5.2

Copyright Clearance Center RightsLink®

Home | Create Account | Help

Title: Trends in fetal monitoring through phonocardiography: Challenges and future directions

Author: Prashanth Chetlur Adithya,Ravi Sankar,Wilfrido Alejandro Moreno,Stuart Hart

Publication: Biomedical Signal Processing and Control

Publisher: Elsevier

Date: March 2017

LOGIN

If you're a copyright.com user, you can login to RightsLink using your copyright.com credentials.

Already a RightsLink user or want to learn more?

Please note that, as the author of this Elsevier article, you retain the right to include it in a thesis or dissertation, provided it is not published commercially. Permission is not required, but please ensure that you reference the journal as the original source. For more information on this and on your other retained rights, please visit: https://www.elsevier.com/about/our-business/policies/copyright#Author-rights

BACK | CLOSE WINDOW

ABOUT THE AUTHOR

Prashanth Chetlur Adithya received his Bachelor of Technology in Electrical Engineering degree from the Jawaharlal Nehru Technological University, Hyderabad, India in 2012; his Masters of Science in Electrical Engineering from the University of South Florida, Tampa, Florida in 2013. He became a Ph.D. student in the Electrical Engineering Department at the University of South Florida in 2014. His doctoral research focused on developing a novel biomedical diagnostic device to improve diagnostic precision in critical and obstetric care. He also contributed to other areas of biomedical research by collaborating with multiple cross-functional teams and by mentoring colleagues and students. His research interests include medical device design and development, biomedical signal processing and modelling, systems engineering, artificial intelligence, embedded systems, and innovation in engineering education.